US 20240009660A1

(19) **United States**

(12) **Patent Application Publication** (10) **Pub. No.: US 2024/0009660 A1**

PARSAPUR et al. (43) **Pub. Date: Jan. 11, 2024**

(54) **METHODS FOR SYNTHESIS OF HIERARCHICALLY ORDERED CRYSTALLINE MICROPOROUS MATERIALS WITH LONG-RANGE MESOPOROUS ORDER**

(71) Applicants: **Saudi Arabian Oil Company**, Dhahran (SA); **King Abdullah University of Science and Technology**, Thuwal (SA)

(72) Inventors: **Rajesh Kumar PARSAPUR**, Thuwal (SA); **Robert Peter HODGKINS**, Dhahran (SA); **Omer Refa KOSEOGLU**, Dhahran (SA); **Kuo-Wei HUANG**, Thuwal (SA); **Anissa Bendjeriou SEDJERARI**, Thuwal (SA)

(21) Appl. No.: **18/151,782**

(22) Filed: **Jan. 9, 2023**

Related U.S. Application Data

(63) Continuation-in-part of application No. 17/857,671, filed on Jul. 5, 2022.

Publication Classification

(51) **Int. Cl.**

B01J 37/10	(2006.01)
B01J 35/10	(2006.01)
B01J 29/08	(2006.01)
C01B 39/24	(2006.01)
B01J 37/04	(2006.01)

(52) **U.S. Cl.**

CPC ***B01J 37/10*** (2013.01); ***B01J 35/1061*** (2013.01); ***B01J 35/1057*** (2013.01); ***B01J 29/084*** (2013.01); ***C01B 39/24*** (2013.01); ***B01J 37/04*** (2013.01); *C01P 2002/72* (2013.01); *C01P 2006/14* (2013.01); *C01P 2006/16* (2013.01)

(57) **ABSTRACT**

Methods for synthesis of hierarchically ordered zeolites and zeolite-type materials are provided. Synthesized hierarchically ordered zeolites and zeolite-type materials formed according to the methods herein possess a high-degree of well-defined long-range mesoporous ordering. The methods include base-mediated reassembly, by dissolution of the parent material to the level of oligomeric structural building units of the parent material, and minimizing or avoiding amorphization/structural collapse. The dissolution and self-assembly is comprehensively controlled to produce hierarchically ordered zeolites and zeolite-type materials according to the methods herein.

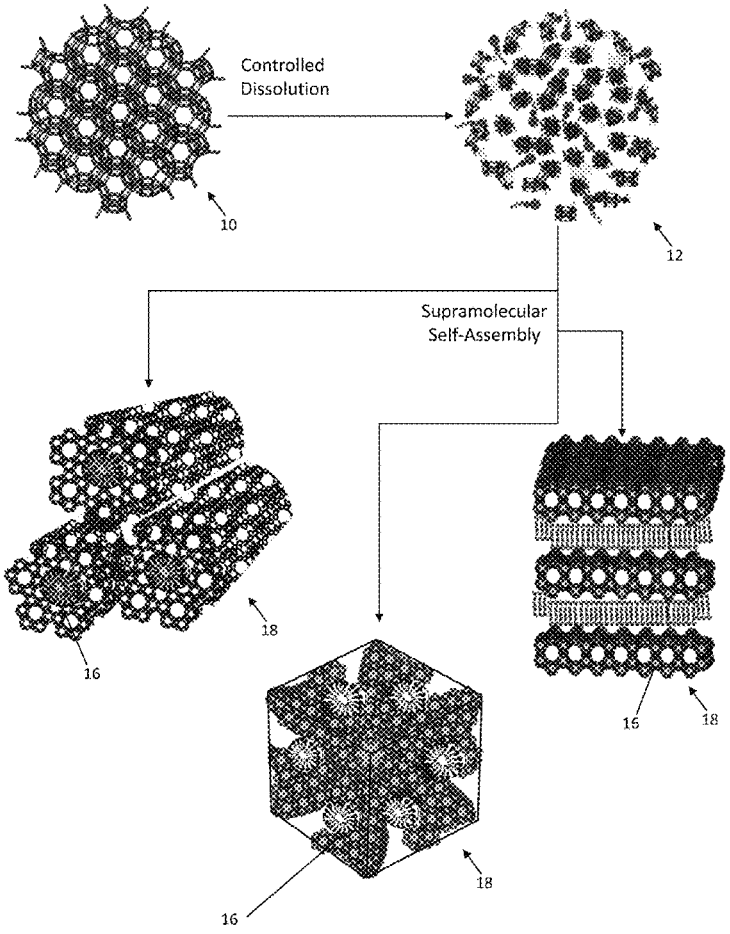

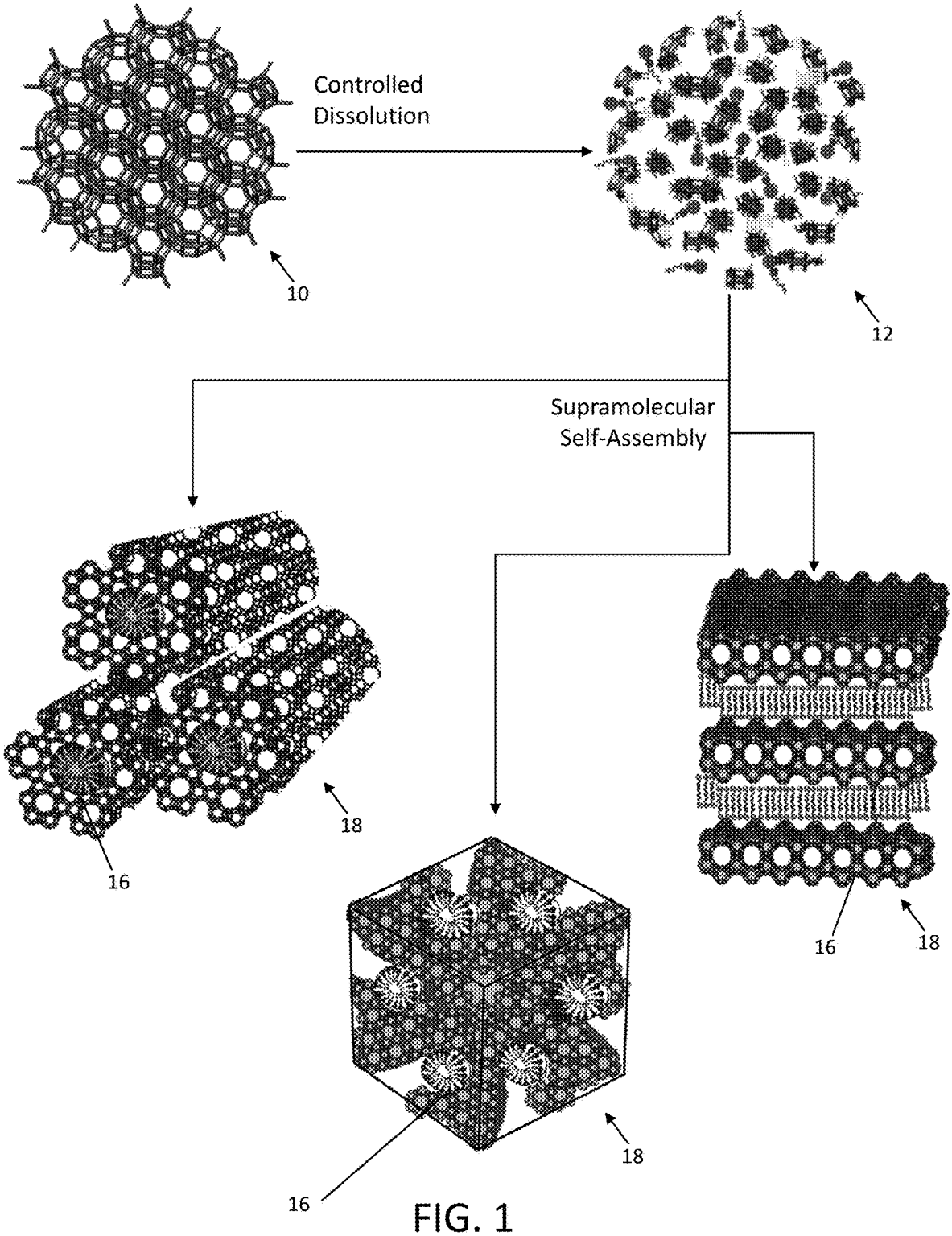
Controlled
Dissolution
10
12
Supramolecular
Self-Assembly
16
18
16
18
16
18

FIG. 1

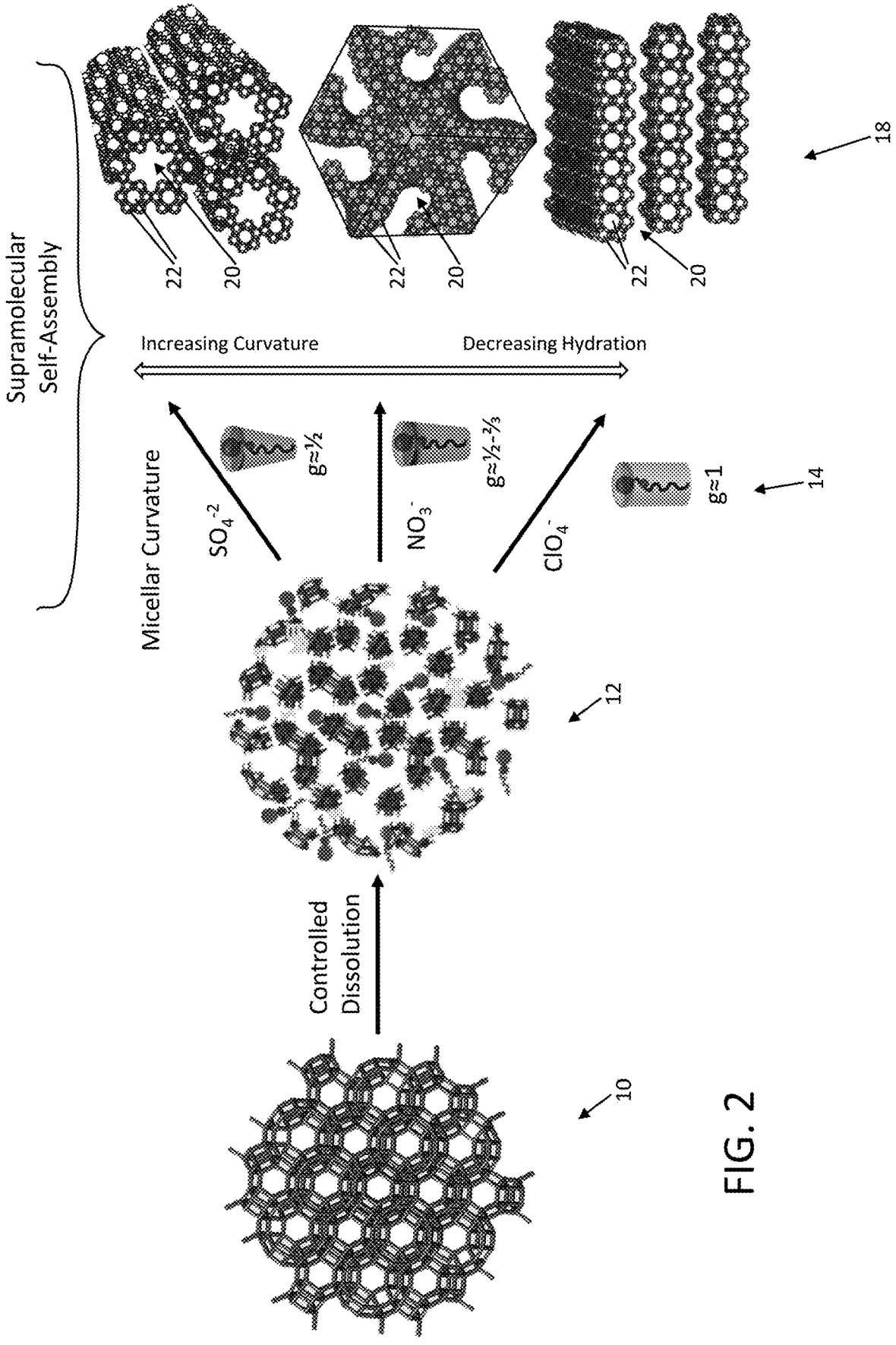
Supramolecular Self-Assembly
Increasing Curvature
Decreasing Hydration
Micellar Curvature
SO_4^{-2}
g≈½
NO_3^-
g≈½-⅔
ClO_4^-
g≈1
Controlled Dissolution
22
20
10
12
14
18

FIG. 2

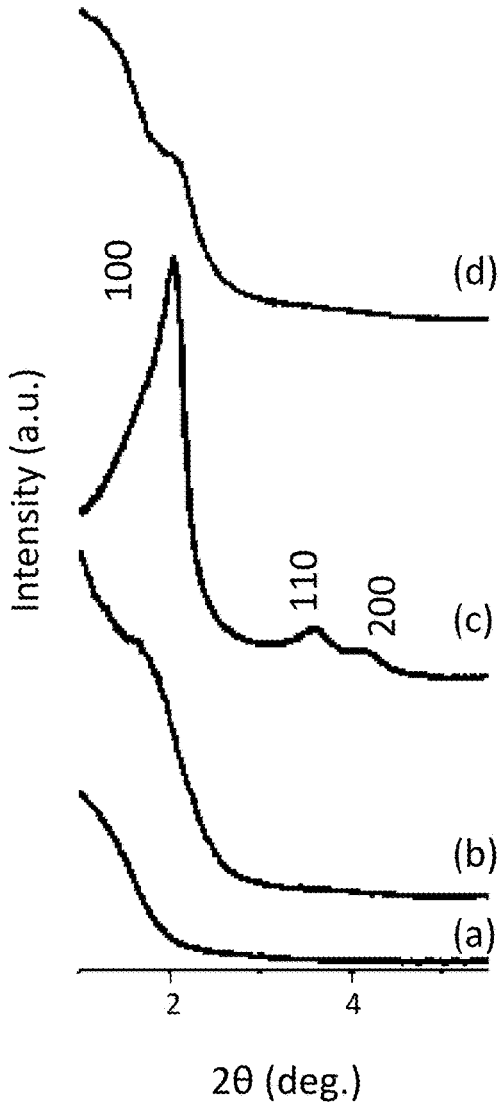
Intensity (a.u.)
100
110
200
(d)
(c)
(b)
(a)
2
4
2θ (deg.)

FIG. 3A

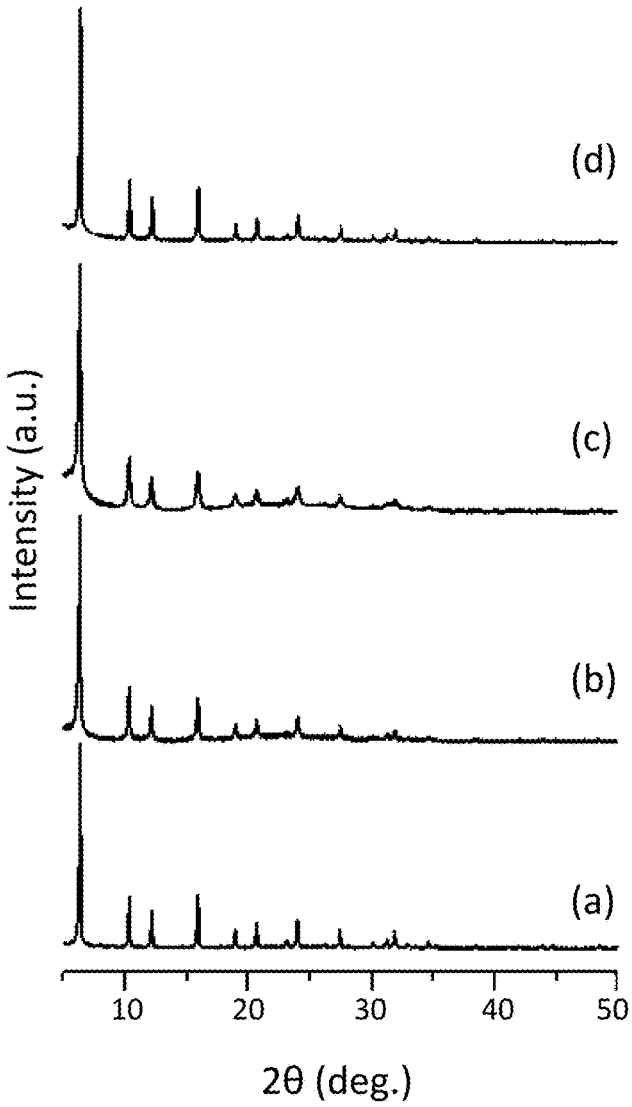
Intensity (a.u.)
(d)
(c)
(b)
(a)
10
20
30
40
50
2θ (deg.)

FIG. 3B

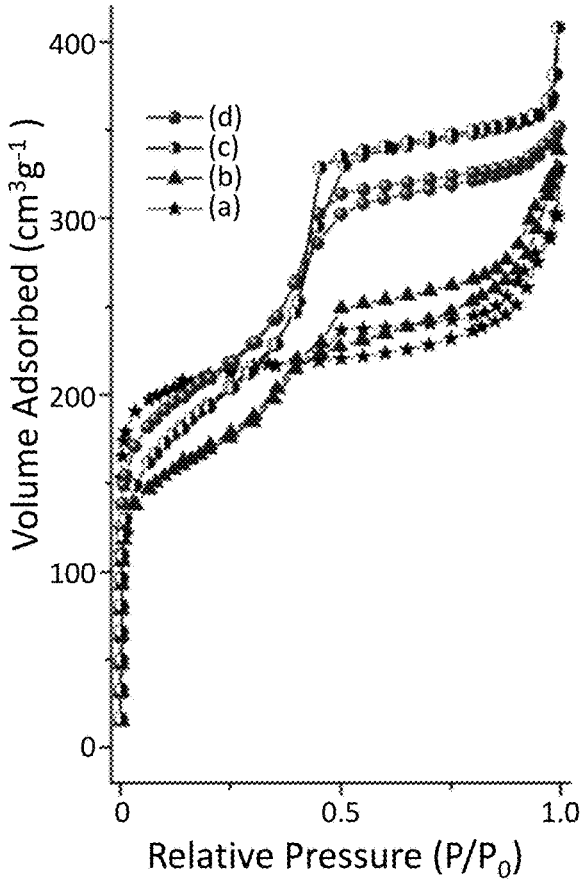
400
300
200
100
0
0
0.5
1.0
Volume Adsorbed (cm^3g^{-1})
Relative Pressure (P/P_0)
(d)
(c)
(b)
(a)

FIG. 4A

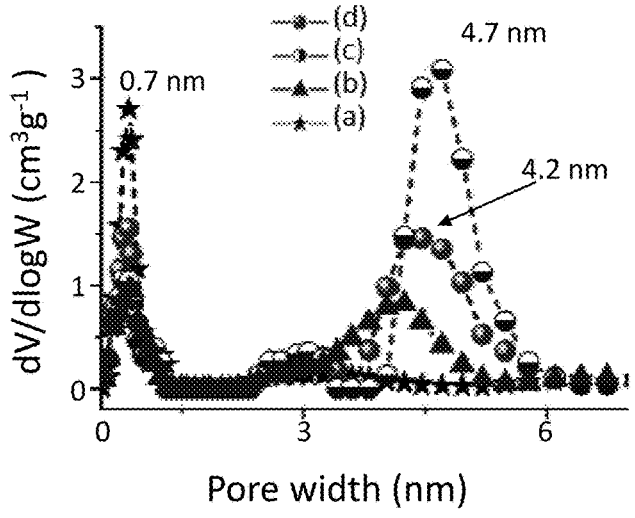
3
2
1
0
0
3
6
dV/dlogW (cm^3g^{-1})
Pore width (nm)
0.7 nm
4.7 nm
4.2 nm
(d)
(c)
(b)
(a)

FIG. 4B

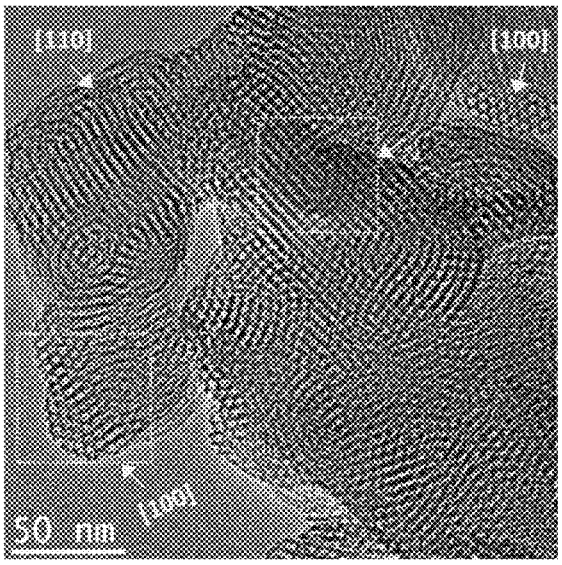

FIG. 5A

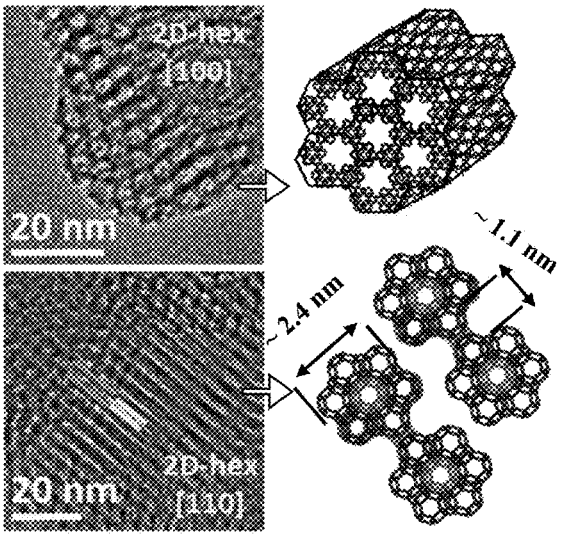

FIG. 5B

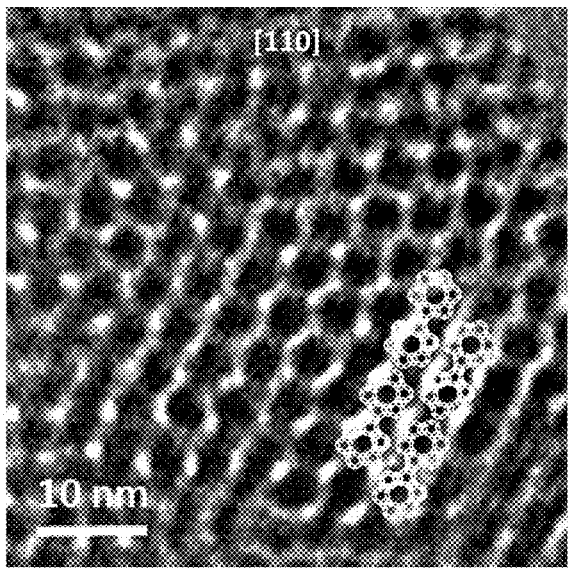

FIG. 5C

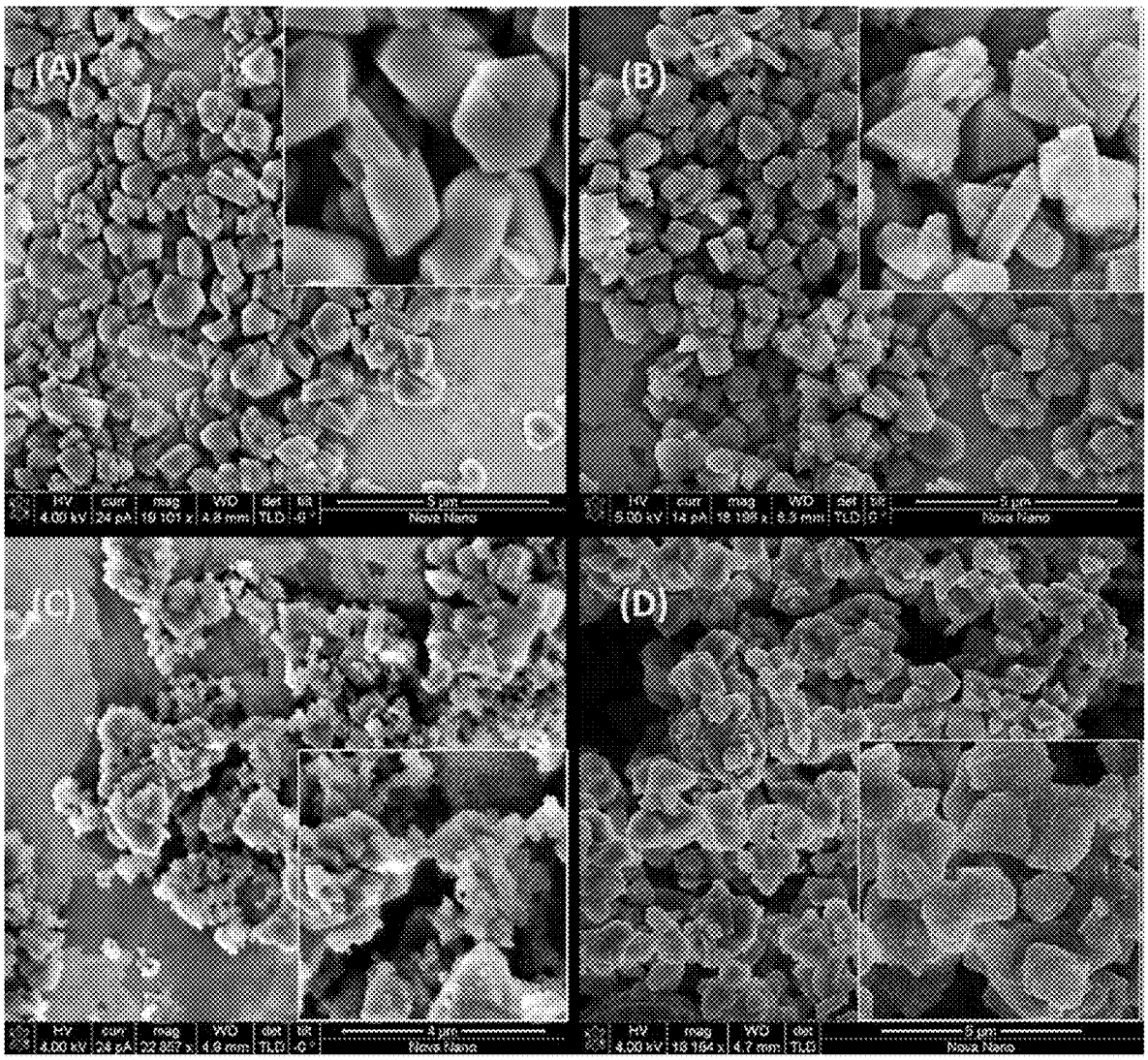

FIG. 6

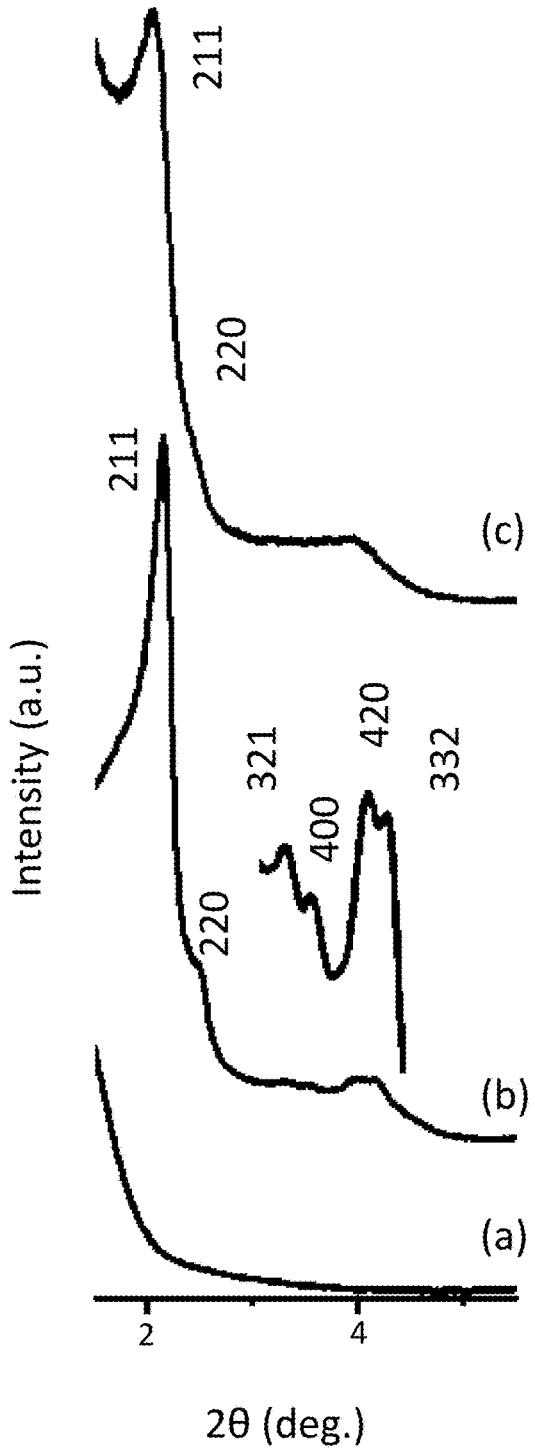
211
220
211
(c)
Intensity (a.u.)
321
420
400
332
220
(b)
(a)
2
4
2θ (deg.)

FIG. 7A

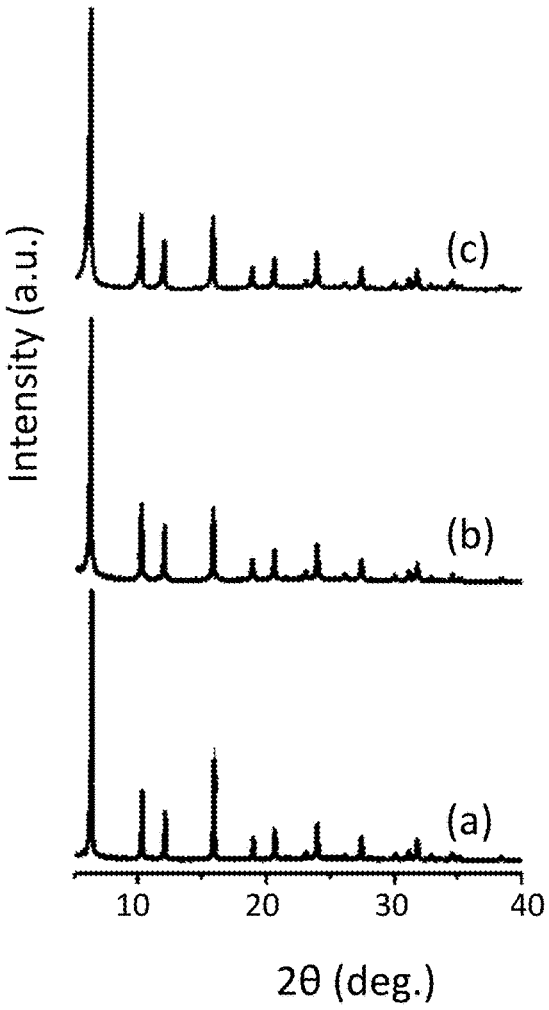
Intensity (a.u.)
(c)
(b)
(a)
10
20
30
40
2θ (deg.)

FIG. 7B

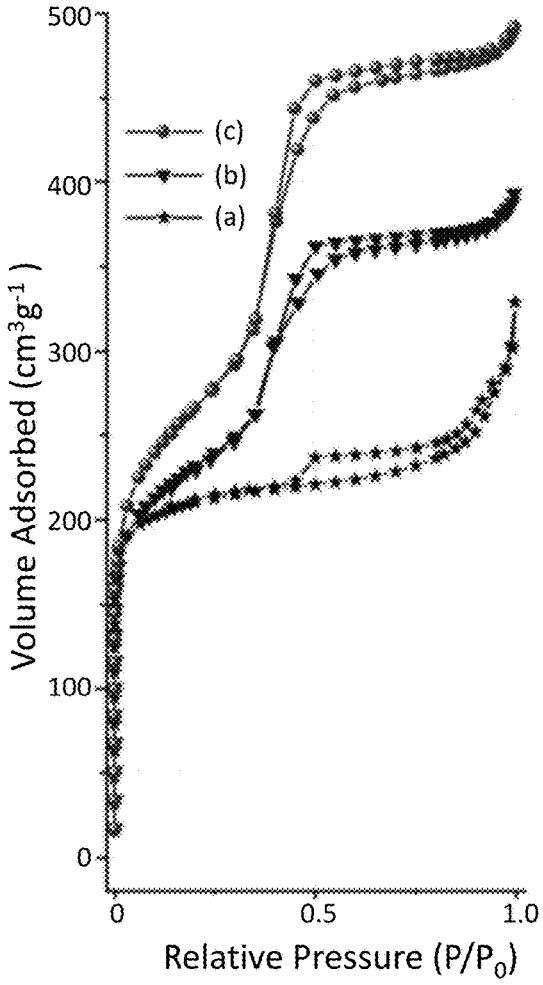
500
400
300
200
100
0
(c)
(b)
(a)
Volume Adsorbed (cm^3g^{-1})
0
0.5
1.0
Relative Pressure (P/P_0)

FIG. 8A

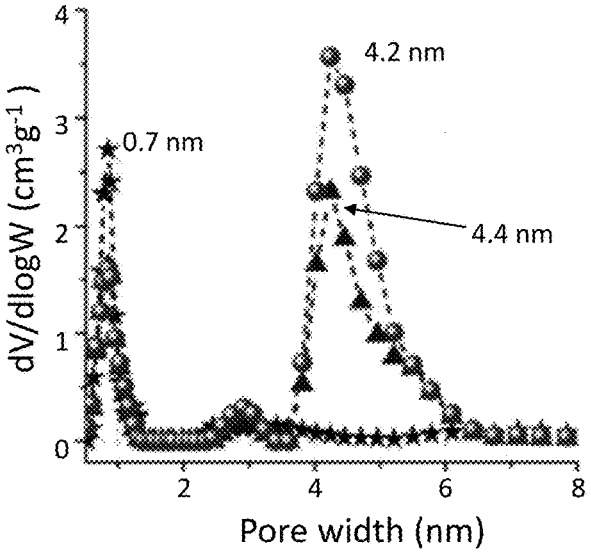
4
3
2
1
0
0.7 nm
4.2 nm
4.4 nm
dV/dlogW (cm^3g^{-1})
2
4
6
8
Pore width (nm)

FIG. 8B

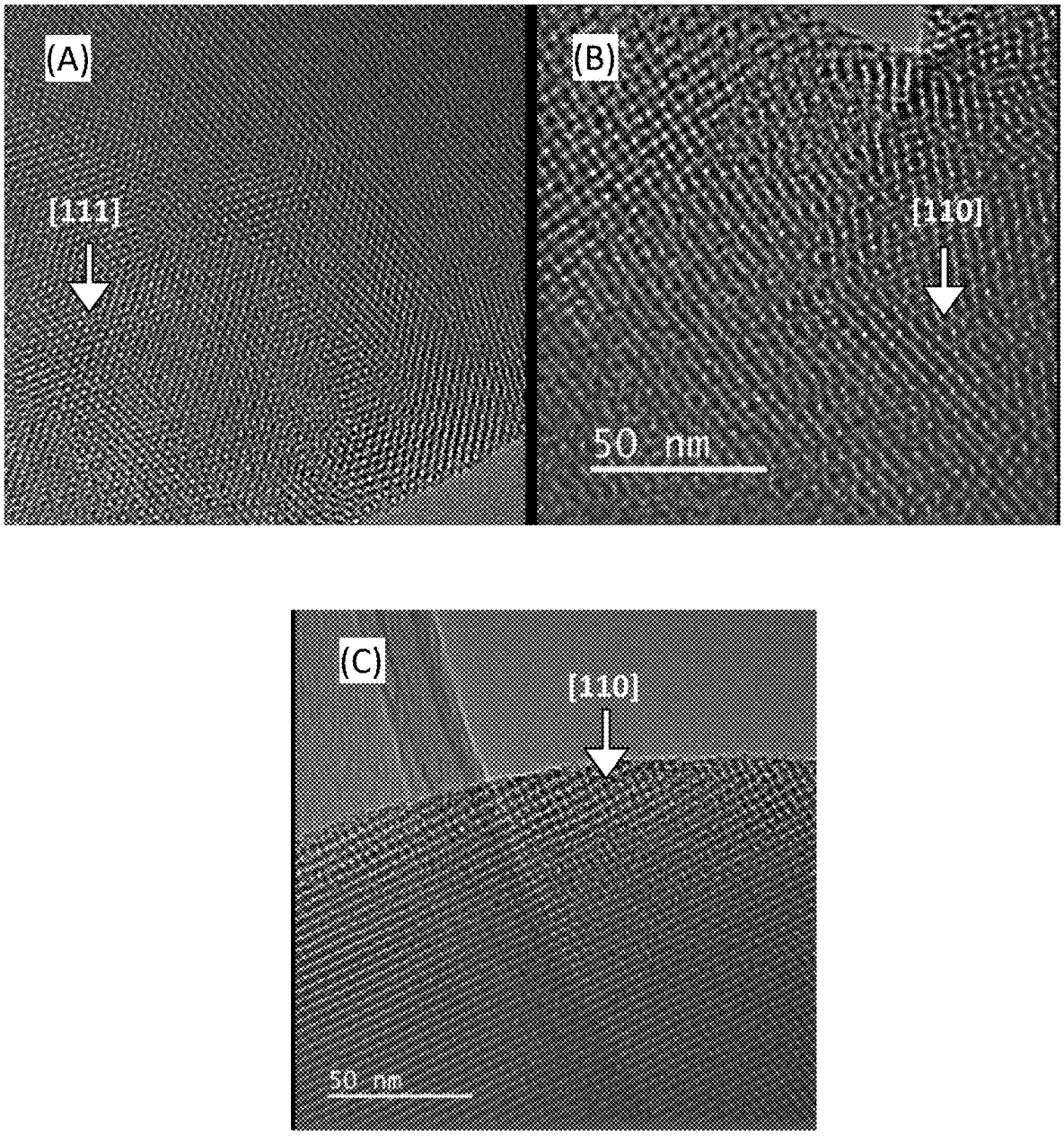

FIG. 9

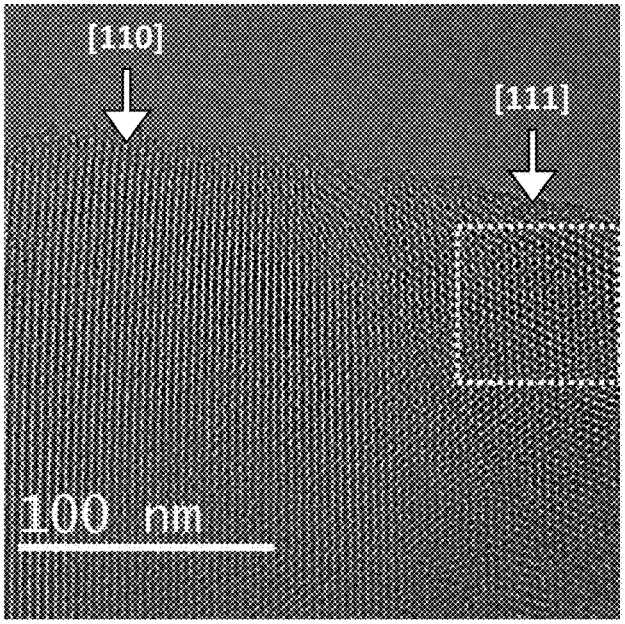

FIG. 10A

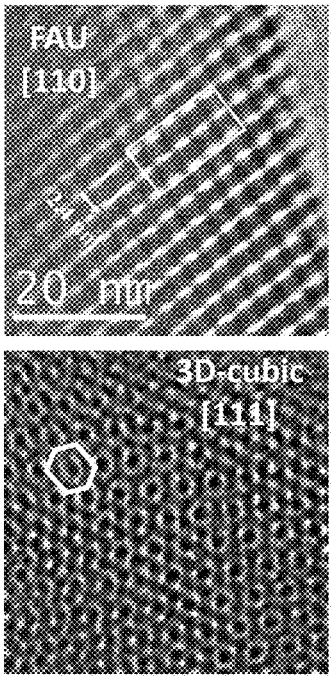

FIG. 10B

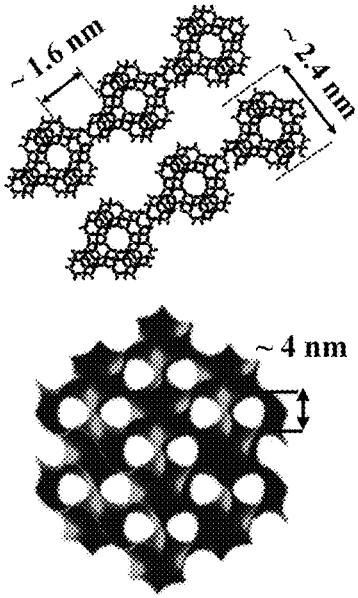

FIG. 10C

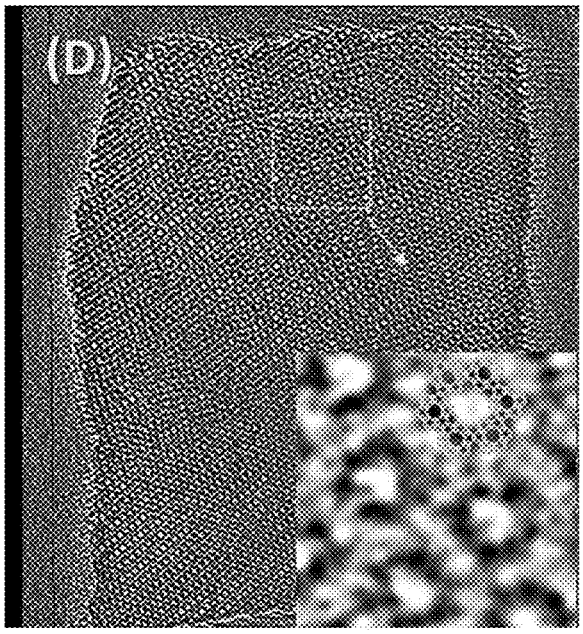

FIG. 11

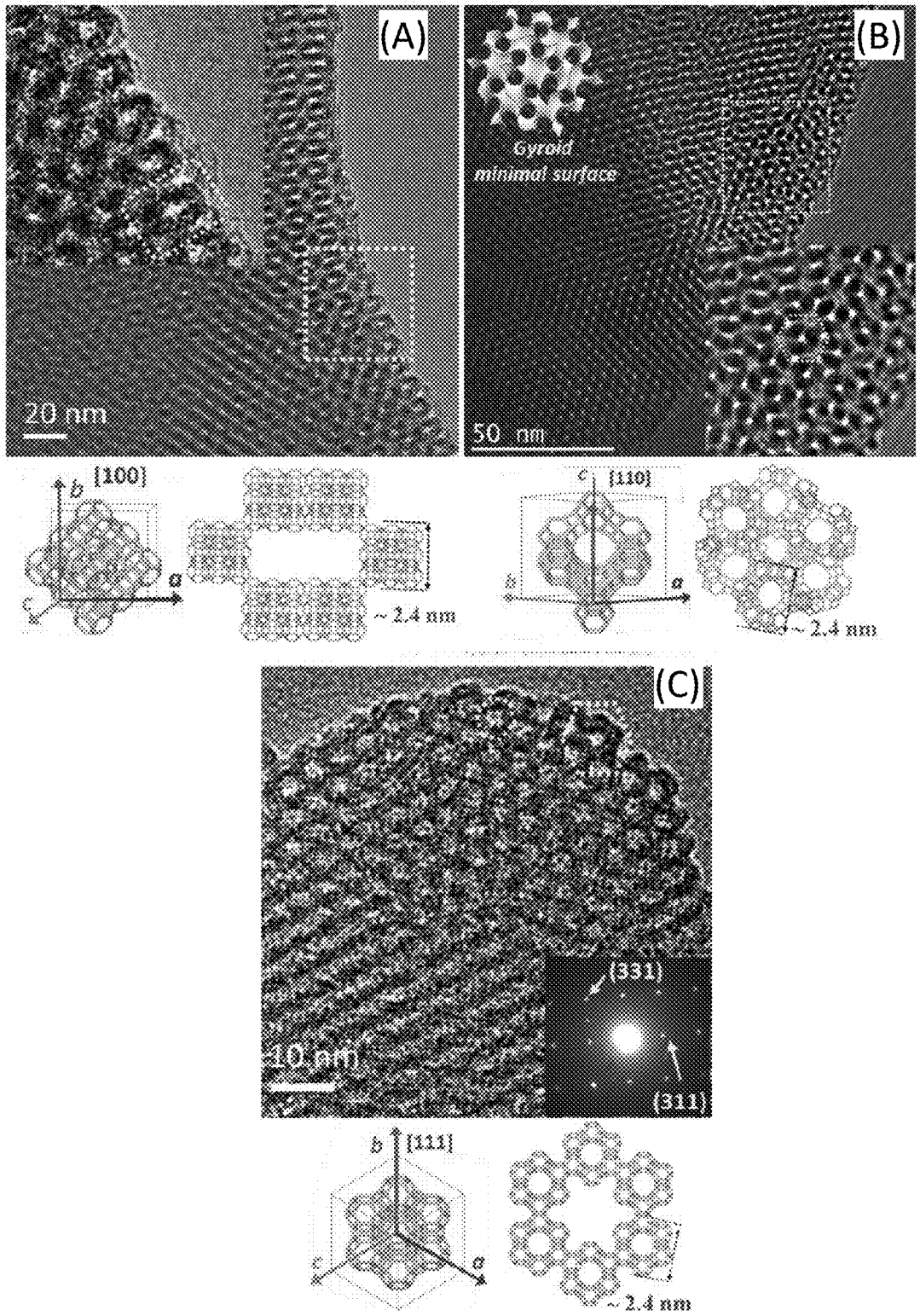
(A)
20 nm
(B)
Gyroid
minimal surface
50 nm
[100]
b
a
~ 2.4 nm
[110]
c
b
a
~ 2.4 nm
(C)
(331)
(311)
10 nm
[111]
b
c
a
~ 2.4 nm

FIG. 12

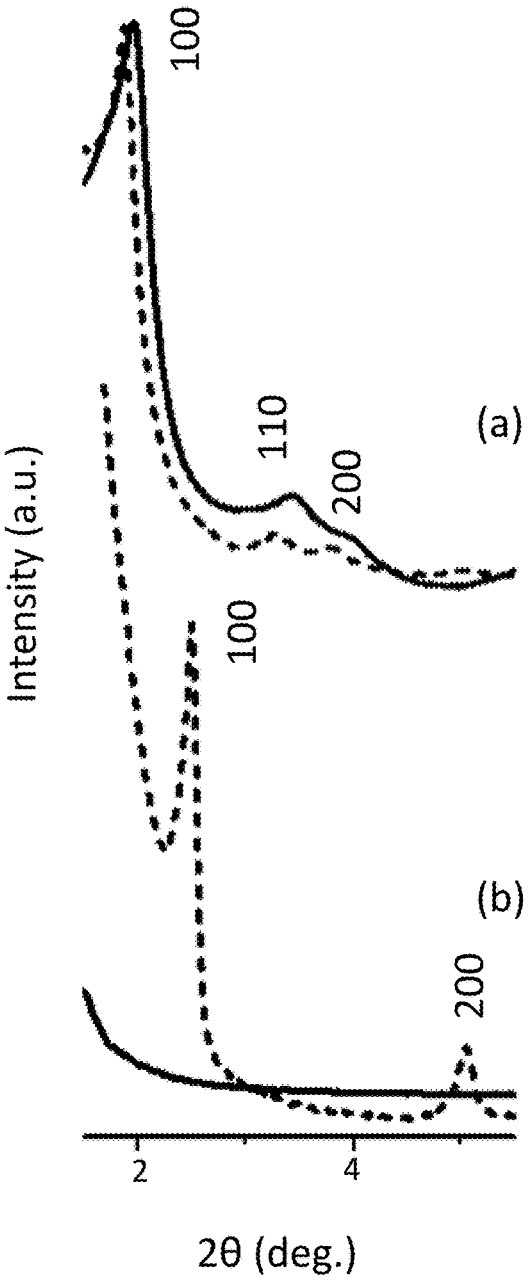

FIG. 13A

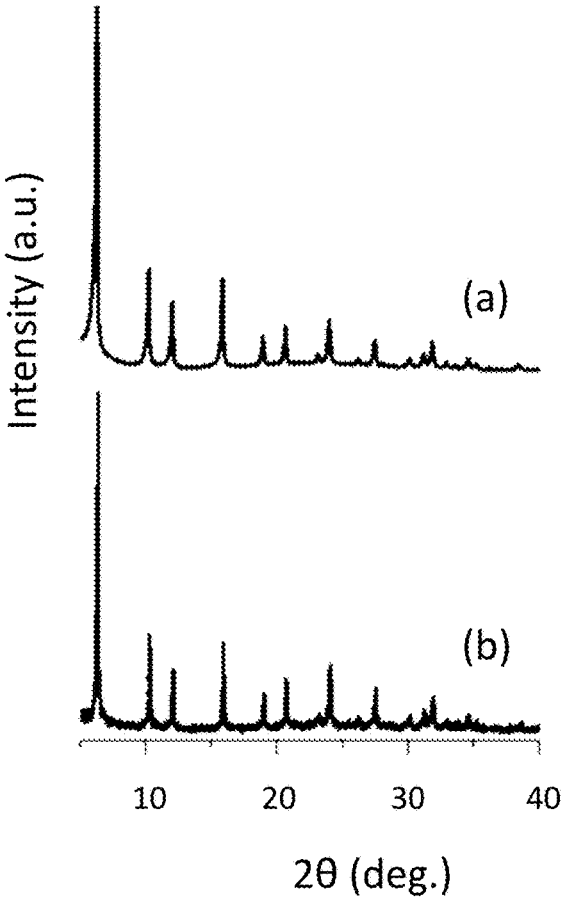

FIG. 13B

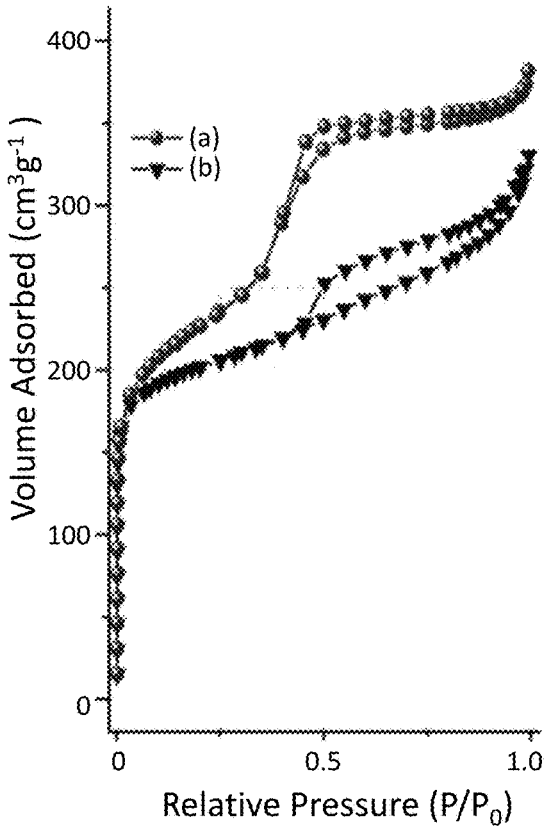

FIG. 14A

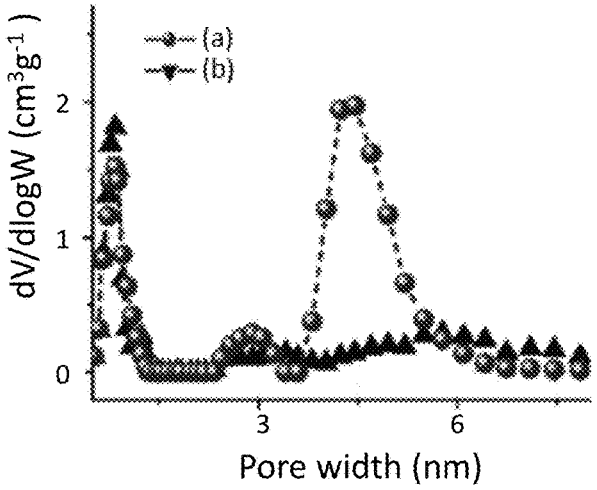

FIG. 14B

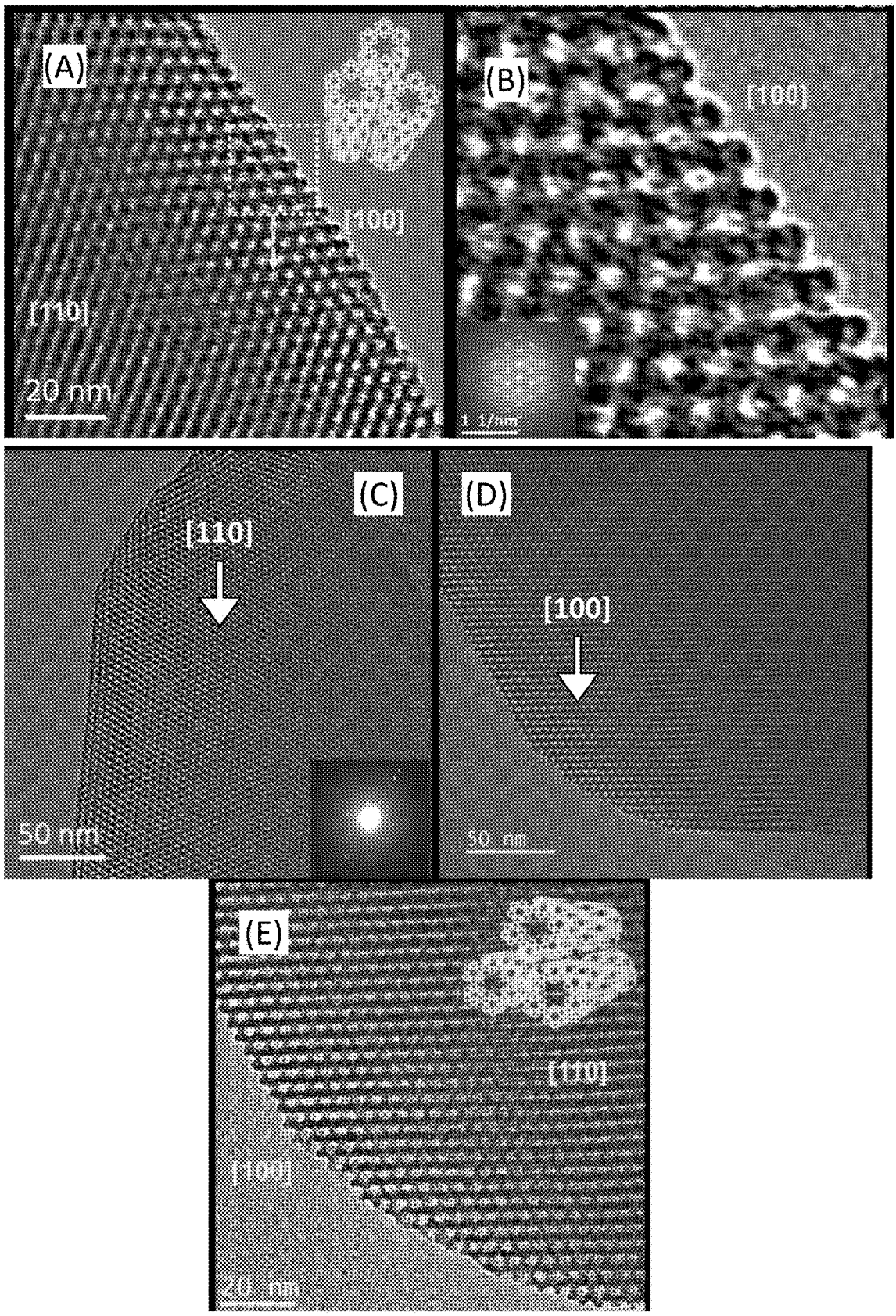

FIG. 15

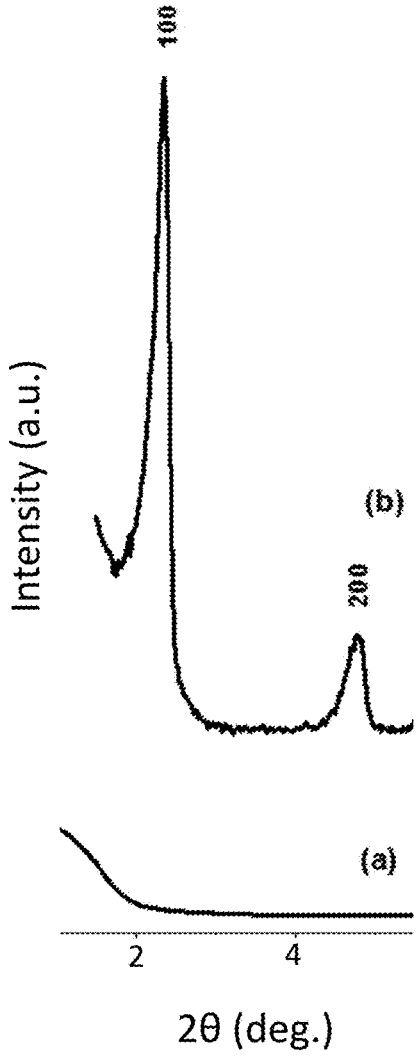

FIG. 16A

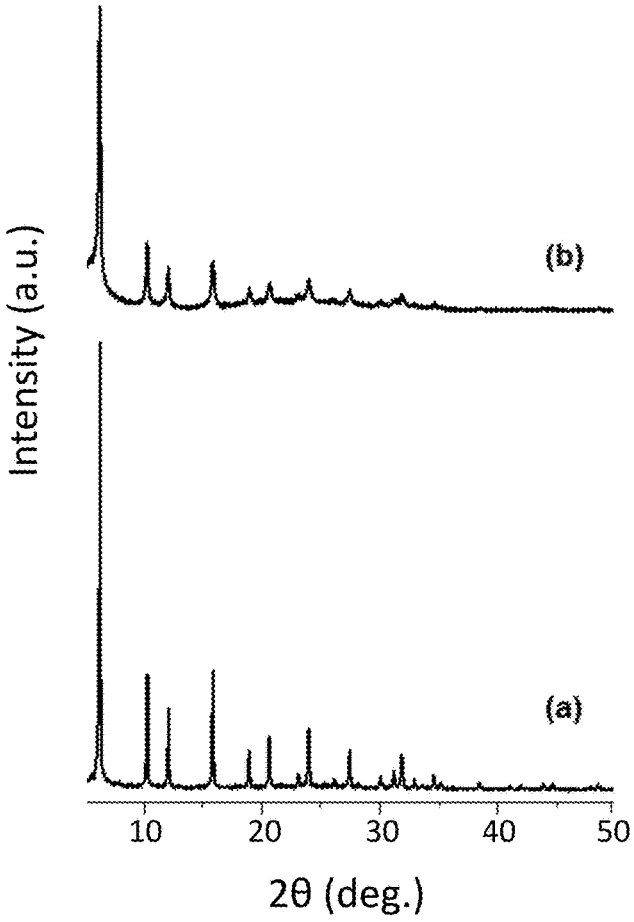

FIG. 16B

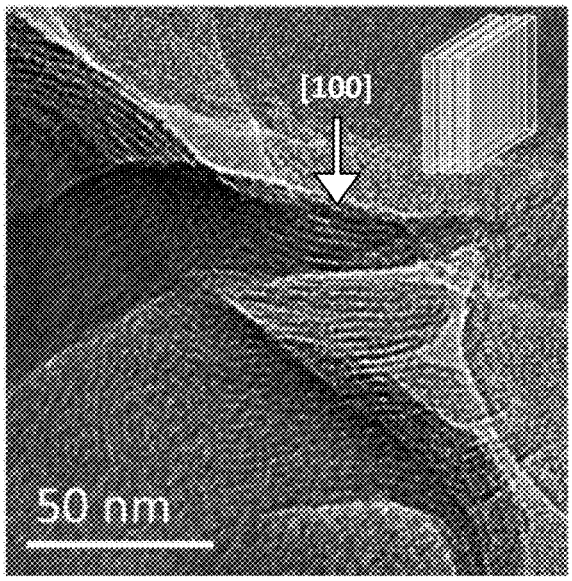

FIG. 17A

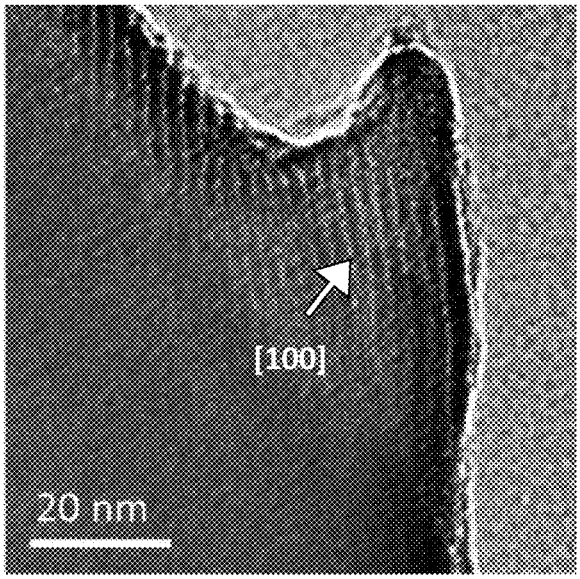

FIG. 17B

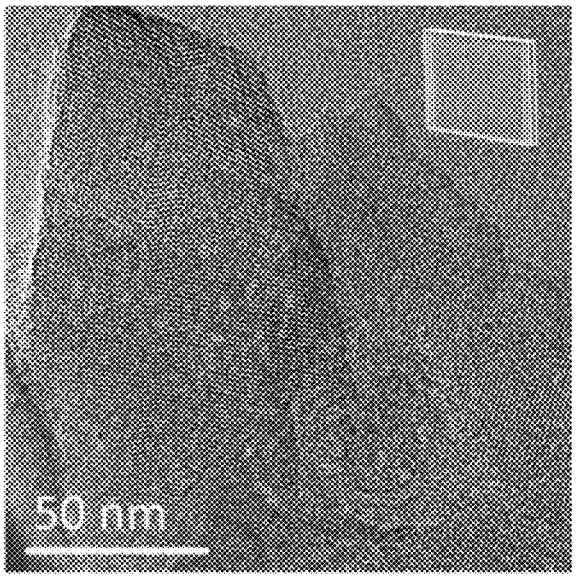

FIG. 17C

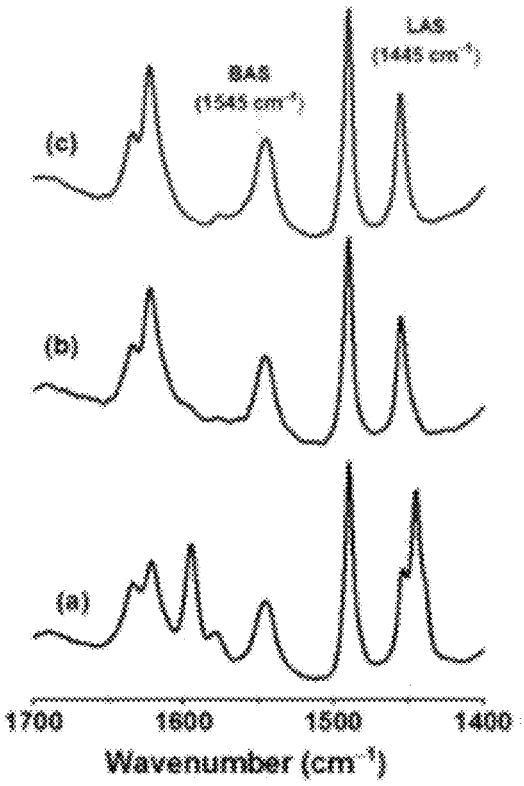

FIG. 18

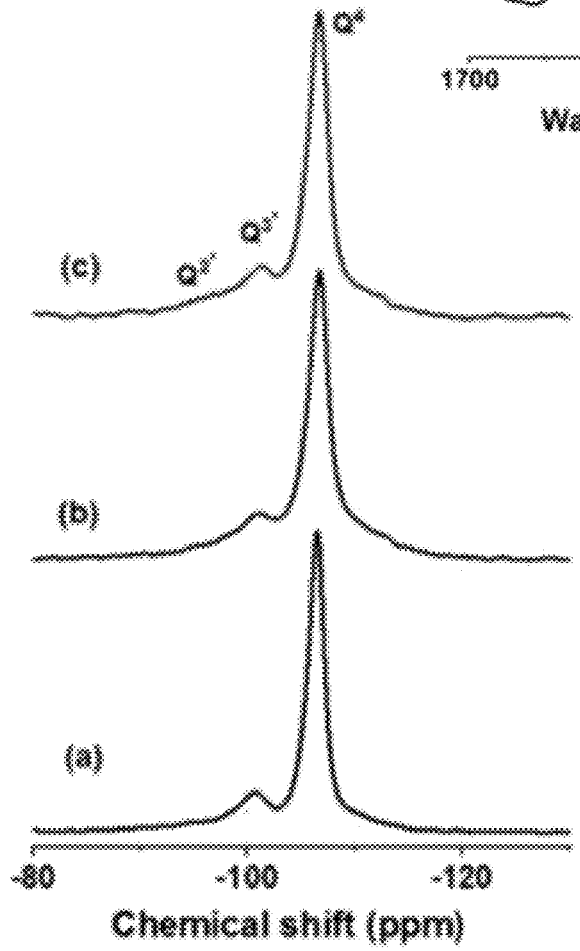

FIG. 19A

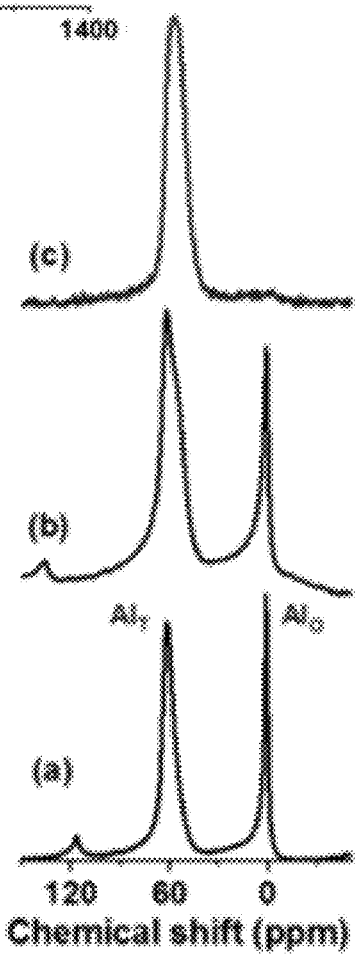

FIG. 19B

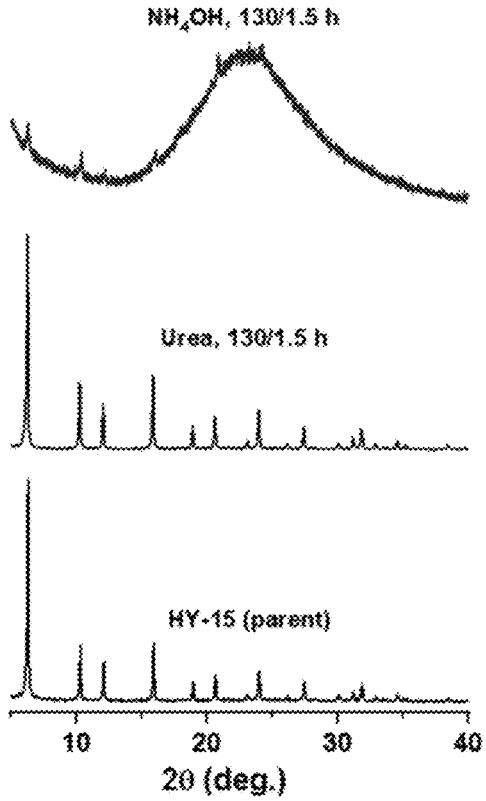

FIG. 20A

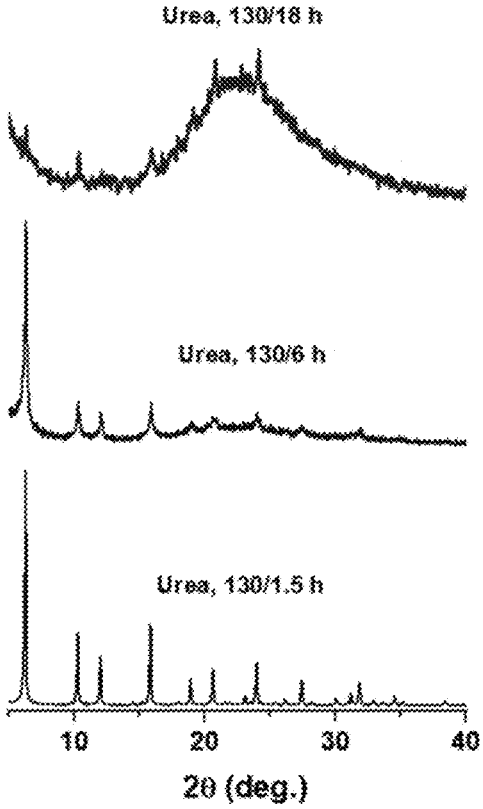

FIG. 20B

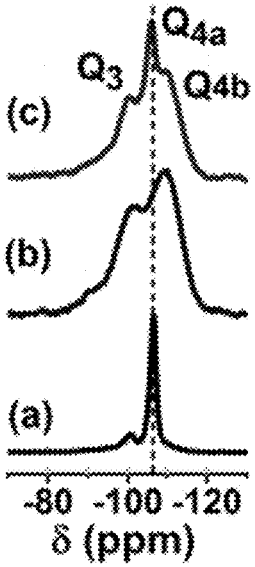

FIG. 20C

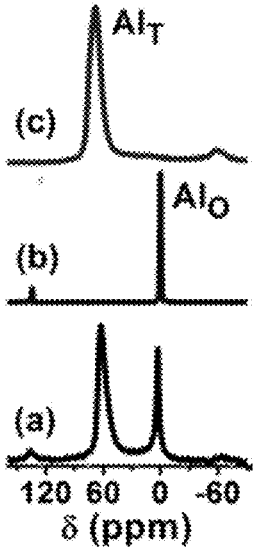

FIG. 20D

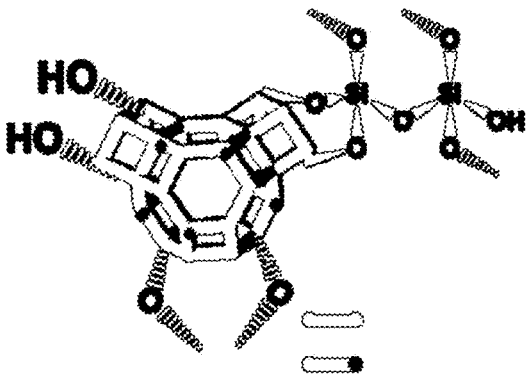

FIG. 20E

METHODS FOR SYNTHESIS OF HIERARCHICALLY ORDERED CRYSTALLINE MICROPOROUS MATERIALS WITH LONG-RANGE MESOPOROUS ORDER

RELATED APPLICATIONS

[0001] This application is a continuation-in-part of U.S. patent application Ser. No. 17/857,671 filed Jul. 5, 2022, the contents of which are is incorporated herein by reference.

FIELD OF THE DISCLOSURE

[0002] The present disclosure relates to methods for synthesis of hierarchically ordered crystalline microporous materials.

BACKGROUND OF THE DISCLOSURE

Zeolites

[0003] Zeolites are microporous aluminosilicate materials possessing well-defined structures and uniform pore sizes that can be measured in nanometers or angstroms (Å) (pores typically up to about 20 Å). Typically, zeolites comprise framework atoms such as silicon, aluminum and oxygen arranged as silica and alumina tetrahedra. Zeolites are generally hydrated aluminum silicates that can be made or selected with a controlled porosity and other characteristics, and typically contain cations, water and/or other molecules located in the porous network. Hundreds of natural and synthetic zeolite framework types exist with a wide range of applications. Numerous zeolites occur naturally and are extensively mined, whereas a wealth of interdependent research has resulted in an abundance of synthetic zeolites of different structures and compositions. The unique properties of zeolites and the ability to tailor zeolites for specific applications has resulted in the extensive use of zeolites in industry as catalysts (e.g., catalytic cracking of hydrocarbons or as components in catalytic convertors), molecular sieves, adsorbents (e.g., drying agents), ion exchange materials (e.g., water softening) and for the separation of gases. Certain types of zeolites find application in various processes in petroleum refineries and many other applications. The zeolite pores can form sites for catalytic reactions, and can also form channels that are selective for the passage of certain compounds and/or isomers to the exclusion of others. Zeolites can also possess an acidity level that enhances its efficacy as a catalytic material or adsorbent, alone or with the addition of active components. Described below is only one of the hundreds of types of zeolites that are identified by the International Zeolite Association (IZA). Properties and uses of many of these are well known.

[0004] Zeolite Y (also known as Na—Y zeolite or Y-type faujasite zeolite) is a well-known material for its zeolites have ion-exchange, catalytic and adsorptive properties. Zeolite Y is also a useful starting material for production of other zeolites such as ultra-stable y-type zeolite (USY). Like typical zeolites, faujasite is synthesized from alumina and silica sources, dissolved in a basic aqueous solution and crystallized. The faujasite zeolite has a framework designated as FAU by the IZA, and are formed by 12-ring structures having made of supercages with pore opening diameters of about 7.4 angstroms (Å) and sodalite cages with pore opening diameters of about 2.3 Å. Faujasite zeolites are characterized by a 3-dimensional pore structure with pores running perpendicular to each other in the x, y, and z planes. Secondary building units can be positioned at 4, 6, 6-2, 4-2, 1-4-4 or 6-6. An example silica-to-alumina ratio (SAR) range for faujasite zeolite is about 2 to about 6, typically with a unit cell size (units a, b and c) in the range of about 24.25 to 24.85 Å. Faujasite zeolites are typically considered X-type when the SAR is at about 2-3, and Y-type when the SAR is greater than about 3, for instance about 3-6. Typically, faujasite is in sodium form and can be ion exchanged with ammonium, and an ammonium form can be calcined to transform the zeolite to its proton form.

Mesoporous Silica

[0005] Whereas zeolites have found great utility in their ability to select between small molecules and different cations, mesoporous solids (pores between about 20 and 500 Å) offer possibilities for applications for species up to an order of magnitude larger in dimensions such as nanoparticles and enzymes. The comparatively bulky nature of such species hinders diffusion through the microporous zeolite network, and thus, a larger porous system is required to effectively perform an analogous molecular sieving action for the larger species.

[0006] Mesoporous silicas are amorphous; however, it is the pores that possess long-range order with a periodically aligned pore structure and uniform pore sizes on the mesoscale. Mesoporous silicas offer high surface areas and can be used as host materials to introduce additional functionality for a diverse range of applications such as adsorption, separation, catalysis, drug delivery and energy conversion and storage.

Ordered Structures

[0007] An attractive property of ordered structures is that their architecture may be described in relation to their symmetry. The regular form of crystals is associated with the regular arrangements of the sub-units comprising the crystal, and hence, the symmetry of the crystal is connected to the symmetry of the sub-units. For example, seven distinct three-dimensional crystal units are provided in Table 1. The crystal systems can be sub-divided upon the symmetry elements present, collectively referred to as the point group and provided in Table 2. For example, 3m infers that a mirror plane having a three-fold axis is present. For the class 3/m (or 6) the mirror plane is perpendicular to the three-fold axis. In 2D space, such as a lamellar system, having fewer dimensions than 3D, there are four crystal systems: hexagonal, square, rectangular and oblique.

Hierarchically Ordered Zeolites

[0008] The well-defined microporous structure of zeolites provides an amalgam of important physicochemical functionalities that are highly desirable in various industrial practices. Their molecular-sized pore channels embedded with tunable acid/base sites can geometrically discriminate the ingress of guest species and direct shape-selective transformations. Such remarkable properties uniquely exhibited by zeolites demonstrate unprecedented importance in numerous chemical technologies, including but not limited to oil-refining, detergents and effluent abatement, that profoundly impact the global economy and environment. However, zeolite performance is often hindered as a result of

their poor mass-transfer abilities induced by configurational diffusion inside the narrow micropores. Therefore, mitigation of the intrinsic mass-transfer limitations is important to explore the full potential of zeolites in diverse energy economies and thereby enhance the accessibility to internal functional sites. Other drawbacks of microporous zeolites as catalysts in certain reactions are their susceptibility to coking, which can lead to accelerated deactivation of catalysts and product selectivity.

[0009] In this regard, hierarchically ordered zeolites (HOZs) possessing an ordered mesoporous structure and zeolitized mesopore walls are of great technological importance due to their exceptional properties. HOZs contain different layers of porosity, that is, mesopores and micropores. Hierarchically ordered zeolites offer advantages over traditional microporous zeolites by, for example, improving diffusion of guest species to the active sites, overcoming steric limitations, improving product selectivity, decreasing coke formation, improving hydrothermal stability, and improving accessibility of Brønsted acid sites and Lewis acid sites; and concomitantly, improved catalytic performance.

[0010] Numerous synthetic strategies to produce hierarchical zeolites are known, and fall under two general categories: bottom-up approaches which include the use of hard templates and soft templates, and top-down approaches which typically involve post-synthetic treatment. Bottom-up strategies generally involve templating techniques used in situ during zeolite crystallization, for example using hard templates (carbon sources) or soft templates (surfactants). Top-down strategies generally involve post-synthetic modifications of already formed zeolite crystals, for example, by steaming, dealumination (using an acid) or desilication (using a base). Weaknesses of known processes to produce hierarchically ordered zeolites is that the long-rage ordering of the mesophase in the resulting zeolite is limited or non-existent, and mesopores can be random in size, location and ordering.

[0011] Base-mediated desilication offers a direct route to creating mesoporosity in high-silica frameworks obtained from steaming. (see, e.g.: Verboekend, D., Milina, M., Mitchell, S. & Perez-Ramirez, J. Hierarchical Zeolites by Desilication: Occurrence and Catalytic Impact of Recrystallization and Restructuring. *Crys. Growth Des.* 13, 5025-5035(2013)). In particular, integrating organic templates during the desilication process has significantly improved crystallinity and mesoporosity. (see, e.g.: García-Martinez, J., Johnson, M., Valla, J., Li, K. & Ying, J. Y. Mesostructured Zeolite Y—High Hydrothermal Stability and Superior FCC Catalytic Performance. *Catal. Sci. Tech.* 2, 987 (2012); Mendoza-Castro, M. J., Serrano, E., Linares, N. & García-Martínez, J. Surfactant-Templated Zeolites: From Thermodynamics to Direct Observation. *Adv. Mater. Interfaces* 8, 2001388 (2020)). However, such post-synthetic modification strategies typically lack control over the dissolution and self-assembly process, resulting in poorly interconnected mesopores. (see, e.g.: Schwieger, W. et al. Hierarchy Concepts: Classification and Preparation Strategies for Zeolite Containing Materials with Hierarchical Porosity. *Chem. Soc. Rev.* 45, 3353-3376, doi:10.1039/c5cs00599j (2016)).

[0012] In view of the prior attempts to produce hierarchically ordered zeolites, there remains a need in the art for improved synthesis methods. It is in regard to these and other problems in the art that the present disclosure is directed to provide a technical solution for an effective method to synthesize and produce hierarchically ordered zeolites having well-defined long-range mesoporous ordering.

SUMMARY OF THE DISCLOSURE

[0013] Methods for synthesis of hierarchically ordered zeolites and zeolite-type materials are provided. Synthesized hierarchically ordered zeolites and zeolite-type materials formed according to the methods herein possess a high-degree of well defined long-range mesoporous ordering. The methods include base-mediated reassembly, by dissolution of the parent material to the level of oligomeric structural building units of the parent material, and minimizing or avoiding amorphization/structural collapse. The dissolution and self-assembly is comprehensively controlled to produce hierarchically ordered zeolites and zeolite-type materials according to the methods herein.

[0014] In certain embodiments a method for synthesis of hierarchically ordered crystalline microporous material is provided whereby, the hierarchically ordered crystalline microporous material possesses a high-degree of long-range mesoporous ordering. A parent crystalline microporous material (CMM) is subjected to dissolution/incision into oligomeric components, which are reorganization into hierarchically ordered mesostructures. An effective amount of a parent CMM (having an underlying microporous structure) is combined with an effective amount of an alkaline reagent and an effective amount of a supramolecular template to form an aqueous suspension. The aqueous suspension is hydrothermally treated under conditions effective to form oligomeric units of the parent CMM, form shaped micelles of the supramolecular template, and induce assembly of the oligomeric units around the shaped micelles. A solid is formed as the hierarchically ordered mesostructures that have a high-degree of long-range mesoporous ordering with pores characterized by crystalline microporous walls that retain the underlying microporous structure.

[0015] In certain embodiments a method for synthesis of hierarchically ordered crystalline microporous material is provided. The process comprises: forming an aqueous suspension of mixing an effective amount of a parent crystalline microporous material having an underlying microporous structure, an effective amount of an alkaline reagent and an effective amount of a supramolecular template; and hydrothermally treating the aqueous suspension under conditions effective for mesophase transition to dissolve/incise parent crystalline microporous material into oligomeric units of the parent crystalline microporous material, form shaped micelles of the supramolecular template, and reorganize the oligomeric units around the shaped micelles into hierarchically ordered mesostructures.

[0016] In certain embodiments, the shape of the micelles is tuned by selection of the supramolecular template. In certain embodiments, the aqueous suspension further comprises an ionic co-solute that is separate from an anion associated with the supramolecular template, and the shape of the micelles is tuned by selection of the supramolecular template and the ionic co-solute. In certain embodiments, an ionic co-solute is selected from the group consisting of $CO3_2^-$, SO_4^{2-}, $S2O_3^{2-}$, $H_2PO_4^-$, F^-, Cl^-, Br^-, NO_3^-, I^-, ClO_4^-, SCN^- and $C_6H_5O_8^{-3}$. In certain embodiments, an ionic co-solute is selected from the group consisting of SO_4^{2-}, NO_3^-, and ClO_4^-. In certain embodiments, an ionic

co-solute comprises NO_3^- and the hierarchically ordered mesostructures possess a cubic mesophase symmetry. In certain embodiments, an ionic co-solute comprises SO_4^{2-} and the hierarchically ordered mesostructures possess a hexagonal mesophase symmetry. In certain embodiments, an ionic co-solute comprises ClO_4^- and the hierarchically ordered mesostructures possess a lamellar mesophase symmetry. In certain embodiments mesophase transition is characterized by a surfactant packing parameter g, $g=V/a_0l$, wherein V=total volume of surfactant tails of the supramolecular template, a_0=area of the head group of the supramolecular template, and l=length of surfactant tail of the supramolecular template. For example: hierarchically ordered mesostructures possessing a cubic mesophase symmetry may be characterized by a surfactant packing parameter g in the range of about 0.4-0.8; hierarchically ordered mesostructures possessing a hexagonal mesophase symmetry may be characterized by a surfactant packing parameter g in the range of about 0.4-0.6; and hierarchically ordered mesostructures possessing a lamellar mesophase symmetry may be characterized by a surfactant packing parameter g in the range of about 0.9-1.1. The amount of ionic co-solute may also be expressed as a molar ratio of supramolecular template to co-solute, for example: the hierarchically ordered mesostructures possessing a cubic mesophase symmetry may be characterized by a molar ratio of supramolecular template to co-solute in the range of about 0.8-1.3; hierarchically ordered mesostructures possessing a hexagonal mesophase symmetry may be characterized by a molar ratio of supramolecular template to co-solute in the range of about 0.8-1.3; and hierarchically ordered mesostructures possessing a lamellar mesophase symmetry may be characterized by a molar ratio of supramolecular template to co-solute in the range of about 0.2-0.7.

[0017] In certain embodiments, the supramolecular templates are bulky surfactants having one or more dimensions larger than dimensions of micropores of the crystalline microporous material to constrain diffusion into micropores of the crystalline microporous material, wherein the dimensions relate to a head group of a surfactant, a tail group of a surfactant, or a co-template. In certain embodiments, a supramolecular template contains least one moiety, as a head group or a tail group, selected from the group consisting of organosilanes, hydroxysilyls, alkoxysilyls, aromatics, branched alkyls, sulfonates, carboxylates, phosphates and combinations comprising one of the foregoing moieties. In certain embodiments, a supramolecular template contains at least one cationic moiety selected from the group consisting of a quaternary ammonium moiety and a phosphonium moiety. In certain embodiments, a supramolecular template contains at least one quaternary ammonium group having a terminal alkyl group with 6-24 carbon atoms. In certain embodiments, a supramolecular template contains two quaternary ammonium groups wherein an alkyl group bridging the quaternary ammonium groups contains 1-10 carbon atoms. In certain embodiments, a supramolecular template contains at least one quaternary ammonium group, and at least one head group moiety selected from the group consisting of organosilanes, hydroxysilyls, alkoxysilyls, aromatics, branched alkyls, sulfonates, carboxylates, phosphates and combinations comprising one of the foregoing moieties. In certain embodiments, a supramolecular template contains at least one quaternary ammonium group, and at least one head group moiety selected from the group consisting of organosilanes, hydroxysilyls, alkoxysilyls, aromatics, branched alkyls, sulfonates, carboxylates, phosphates and combinations comprising one of the foregoing moieties, wherein an alkyl group bridging at least one of the quaternary ammonium groups and at least one of the head groups contains 1-10 carbon atoms. In certain embodiments, a supramolecular template comprises dimethyloctadecyl(3-trimethoxysilyl-propyl)-ammonium or a derivative of dimethyloctadecyl(3-trimethoxysilyl-propyl)-ammonium.

[0018] In certain embodiments, the alkaline reagent is provided at a concentration in the aqueous suspension of about 0.1-5 wt % and is selected from the group consisting of ammonia, ammonium hydroxide and urea. In certain embodiments, the alkaline reagent is urea, wherein during hydrothermal treatment, urea reacts to form ammonium hydroxide, thereby controlling hydrothermal treatment.

[0019] In certain embodiments, the as-formed hierarchically ordered mesostructures are calcined. In certain embodiments, the method reduces the amorphous content of the hierarchically ordered mesostructures.

[0020] In certain embodiments, the parent CMM comprises a zeolite or zeolite-type material. In certain embodiments, the parent CMM comprises a zeolite having a framework selected from the group consisting of AEI, *BEA, CHA, FAU, MFI, MOR, LTL, LTA and MWW. The parent CMM comprises a zeolite having FAU framework.

[0021] Any combinations of the various embodiments and implementations disclosed herein can be used. These and other aspects and features can be appreciated from the following description of certain embodiments and the accompanying drawings and claims.

BRIEF DESCRIPTION OF THE DRAWINGS

[0022] The process of the disclosure will be described in more detail below and with reference to the attached drawings in which the same number is used for the same or similar elements.

[0023] FIGS. **1** and **2** are schematic overviews of hierarchical ordering by post-synthetic ensembles synthesis route described herein.

[0024] FIG. **3**A depicts low-angle XRD, and FIG. **3**B depicts high-angle XRD patterns, associated with products synthesized in Examples 1A-1C.

[0025] FIG. **4**A depicts N2 physisorption isotherms, and FIG. **4**B depicts NLDFT pore-size distributions, associated with products synthesized in Examples 1A-1C.

[0026] FIGS. **5**A-C depict TEM micrographs of hierarchically ordered zeolite synthesized in Example 1B.

[0027] FIG. **6** depicts SEM images of products synthesized in Examples 1A-1C.

[0028] FIG. **7**A depicts low-angle XRD, and FIG. **7**B depicts high-angle XRD patterns, associated with products synthesized in Examples 2A-2B.

[0029] FIG. **8**A depicts N2 physisorption isotherms, and FIG. **8**B depicts NLDFT pore-size distributions, associated with products synthesized in Example 2A-2B.

[0030] FIG. **9** depicts TEM micrographs of hierarchically ordered zeolite synthesized in Example 2A.

[0031] FIGS. **10**A-B depict TEM micrographs of hierarchically ordered zeolite synthesized in Example 2A, and FIG. **10**C depicts unit cell schematic and dimensions for parent zeolite.

[0032] FIG. **11** depicts electron tomography reconstruction of hierarchically ordered zeolite synthesized in Example 2B.

[0033] FIG. **12** depicts TEM micrographs of hierarchically ordered zeolite synthesized in Example 2B.

[0034] FIG. **13**A depicts low-angle XRD, and FIG. **13**B depicts high-angle XRD patterns, associated with products synthesized in Examples 3A-3B.

[0035] FIG. **14**A depicts N2 physisorption isotherms, and FIG. **14**B depicts NLDFT pore-size distributions, associated with products synthesized in Example 3A-3B.

[0036] FIG. **15** depicts TEM micrographs of hierarchically ordered zeolite synthesized in Example 3A.

[0037] FIGS. **16**A-B depicts low-angle and high-angle XRD patterns associated with as-made products from Example 4A.

[0038] FIGS. **17**A-C depict TEM micrographs of as-made hierarchically ordered zeolite from Example 4A.

[0039] FIG. **18** depicts an FTIR spectra characterizing acid sites of certain examples herein.

[0040] FIGS. **19**A-B depict a NMR spectra characterizing certain examples herein.

[0041] FIG. **20**A depicts high-angle XRD patterns of the parent zeolite treated with NH_4OH and urea, FIG. **20**B depicts the parent zeolite treated with urea over time, FIGS. **20**C-D depict NMR spectra of the parent zeolite treated with NH_4OH and urea, and FIG. **20**E is a schematic a schematic of zeolitic fragments from urea dissolution.

DETAILED DESCRIPTION OF CERTAIN EMBODIMENTS OF THE DISCLOSURE

[0042] Methods for synthesis of hierarchically ordered zeolites and zeolite-type materials (hereinafter "crystalline microporous material" or "CMM," used in singular or plural forms as appropriate) are provided. Synthesized hierarchically ordered crystalline microporous materials ("HOCMM" used in singular or plural forms as appropriate) formed according to the methods herein possess a high-degree of well-defined long-range mesoporous ordering. Synthesizing HOCMMs in the process herein overcomes problems associated with known methods by using by base-mediated reassembly, by dissolution of the parent CMM to the level of structural building units that are oligomers of the parent CMM, and minimizing or avoiding amorphization/structural collapse. The CMM dissolution and self-assembly is comprehensively controlled to produce HOCMMs according to the methods herein. Compositions formed according to methods disclosed herein are disclosed in co-pending and commonly owned U.S. patent application Ser. No. 17/857,447 filed on Jul. 5, 2022 entitled "Hierarchically Ordered Crystalline Microporous Materials with Long-Range Mesoporous Order Having Cubic Symmetry"; Ser. No. 17/857,503 filed on Jul. 5, 2022 entitled "Hierarchically Ordered Crystalline Microporous Materials with Long-Range Mesoporous Order Having Hexagonal Symmetry"; and Ser. No. 17/857,572 filed on Jul. 5, 2022 entitled "Hierarchically Ordered Crystalline Microporous Materials with Long-Range Mesoporous Order Having Lamellar Symmetry", which are all incorporated by reference herein.

[0043] In certain embodiments of reassembly: the rate and extent of CMM dissolution is controlled by employing urea as an in situ base, and by mediating hydrothermal temperature to control urea hydrolysis and fine-tune pH of the solution; extent of dissolution into smaller oligomers is controlled by the surfactant-CMM interactions during the initial stages of dissolution, whereby influence of the ion-specific interactions, that is, anionic Hofmeister effect (AHE) on supramolecular self-assembly directs formation of hierarchically ordered structures with hexagonal mesopore symmetry, bicontinuous gyroid cubic mesopore symmetry and lamellar symmetry; in certain embodiments the hierarchically ordered structures possess hexagonal P6 mm mesopore symmetry, bicontinuous gyroid cubic Ia-3d mesopore symmetry and lamellar p2 symmetry.

[0044] According to an embodiment of the method, a parent CMM is formed into an aqueous suspension with an alkaline reagent and a supramolecular templating agent. In additional embodiments, the aqueous suspension includes an ionic co-solute as an additional anion that is separate from the anion which is paired with the cation of the supramolecular template. The system is maintained under conditions to induce incision of the parent CMM into oligomeric units of the CMM, with only a minor portion of monomeric units, and to induce hierarchical reassembly of the oligomeric units into mesostructures. System conditions (including temperature and time of crystallization), selection and concentration of supramolecular template, and selection and concentration of alkaline reagent are tailored to control incision of the parent CMM into oligomeric units and to control reassembly of those oligomeric units around the shape(s) of supramolecular template micelles. Dissolution of parent CMM is encouraged to the extent of oligomer formation while minimizing monomer formation, which is controlled by selection of supramolecular template, alkaline reagent, optional ionic co-solute and hydrothermal conditions (including temperature and time). In certain embodiments, a substantial portion, a significant portion or a major portion of the parent CMM is cleaved into oligomeric units, with any remainder in the form of monomeric units or atomic constituents of the CMM. In certain embodiments, dimensions of the oligomeric units correspond approximately to the wall thickness of the synthesized mesoporous structure, the HOCMM. In certain embodiments interface curvature(s) of the micelles and oligomeric units under reassembly is tuned to a desired mesostructure and mesoporosity with the aid of optional ionic co-solute and the Hofmeister effect.

[0045] Under effective crystallization conditions and time, and using effective type(s) of supramolecular template and alkaline reagent at effective relative concentrations, hierarchical ordering by post-synthetic ensembles occurs: the parent CMM is incised into oligomeric CMM units that rearrange around the shaped micelles formed by the supramolecular templates. Hierarchically ordered CMMs having well-defined long-range mesoporous ordering are formed by the supramolecular templating method using the surfactant micelles. The mesopore walls are characterized by the parent CMM. The effective supramolecular templates include those having one or more properties forming a dimension that blocks all, a substantial portion, a significant portion or a major portion of the supramolecular template molecules from entering pores, channels and/or cavities of the parent CMM. These methods disclosed herein effectuate base-mediated incisions of the CMM crystals, in the presence of the supramolecular template of the type/characteristic disclosed herein, into oligomeric components, with subsequent reorganization around well-defined micelles by supramolecular templating, into hierarchically ordered structures having a well-defined long-range mesoporous ordering.

[0046] The curvature or shape of the micelles results in the final mesophase symmetry, for example, hexagonal, cubic or lamellar. Formation of the supramolecular template molecules into micelles is dependent upon factors such as the supramolecular template type, supramolecular template concentration, presence or absence of an ionic co-solute, CMM type(s), crystallization temperature, type of alkaline reagent, concentration of alkaline reagent, pH level of the system, and/or presence or absence of other reagents. In general, at low concentrations supramolecular templates exist as discrete entities. At higher concentrations, that is, above a critical micelle concentration (CMC), micelles are formed. The hydrophobic interactions in the system including the supramolecular template alters the packing shape of the supramolecular templates into, for example, spherical, prolate or cylindrical micelles, which can thereafter form thermodynamically stable two-dimensional or three-dimensional liquid crystalline phases of ordered mesostructures (see, for example, FIG. 1.4 of Zana, R. (Ed.). (2005). Dynamics of Surfactant Self-Assemblies: Micelles, Microemulsions, Vesicles and Lyotropic Phases (1^{st} ed.). CRC Press, Chapter 1, which shows self-assembly based on surfactant and surfactant packing parameter).

[0047] In certain embodiments, the Hofmeister series (HS), ion specific effect, or lyotropic sequence is followed for selection of supramolecular templates and/or ionic co-solute to control curvature or shape (e.g., spherical, ellipsoid, cylindrical, or unilamellar structures) of the micelles (see, for example, Beibei Kang, Huicheng Tang, Zengdian Zhao, and Shasha Song. "Hofmeister Series: Insights of Ion Specificity from Amphiphilic Assembly and Interface Property" ACS Omega 5 (2020): 6229-6239). In embodiments of the methods for synthesis of hierarchically ordered microporous crystalline materials having well-defined long-range mesoporous ordering disclosed herein, mesophase transitions of hierarchical ensembles yield distinct mesostructures based on the anionic Hofmeister effect and supramolecular self-assembly. Anions of different sizes and charges possess different polarizabilities, charge densities and hydration energies in aqueous solutions. When paired with a positive supramolecular template head group, these properties can affect the short-range electrostatic repulsions among the head groups and hydration at the micellar interface, thus changing the area of the head group (a_0). Such ion-specific interactions can be a driving force in changing the micellar curvature and inducing mesophase transition. Based on the HS (SO_4^{2-}>HPO_4^{2-}>Oac^->Cl^->Br^->NO_3^->ClO_4^->SCN^-), strongly hydrated ions (left side of the HS) can increase the micellar curvature, whereas weakly hydrated ions can decrease the micellar curvature. A surfactant packing parameter, g=V/a_0l (V=total volume of surfactant tails, a_0=area of the head group, l=length of surfactant tail), can be used to describe these mesophase transitions.

[0048] In the methods for synthesis of hierarchically ordered CMMs having well-defined long-range mesoporous ordering disclosed herein, suitable alkaline reagents include one or more basic compounds to maintain the system at a pH level of greater than about 8. In certain embodiments the alkaline reagent is provided at a concentration in the aqueous suspension of about 0.1-2.0 M. In certain embodiments the alkaline reagent is provided at a concentration in the aqueous suspension of about 0.1-5 wt %. In certain embodiments the alkaline reagent comprises urea. In certain embodiments the alkaline reagent comprises ammonia. In certain embodiments the alkaline reagent comprises ammonium hydroxide. In certain embodiments the alkaline reagent comprises sodium hydroxide. In certain embodiments the alkaline reagent comprises alkali metal hydroxides including hydroxides of sodium, lithium, potassium, rubidium, or cesium.

[0049] In certain embodiments the alkaline reagent is effective to enable controlled hydrolysis; for example, urea can be used as an alkaline agent, and during hydrolysis urea reacts to form ammonium hydroxide. For example, higher urea concentration can be used in the initial step, and basicity can be maintained by gradual urea hydrolysis. In such embodiments, pH is increased relatively slowly to a maximum pH as a function of time, which is beneficial to the process, rather than adding an amount of another alkaline reagent such as ammonium hydroxide in the initial solution to the maximum pH. Unlike conventional bases, which act swiftly, urea is pH neutral at ambient conditions and can disperse uniformly throughout the zeolitic micropores without affecting them.

[0050] In certain embodiments the alkaline reagent comprises alkylammonium cations, having the general formula $R_XH_{4-X}N^+[A^-]$, wherein at X=1-4 and R_1, R_2, R_3 and R_4 can be the same or different C1-C30 alkyl groups, and wherein $[A^-]$ is a counter anion can be OH^-, Br^-, Cl^- or I^-. In certain embodiments the alkaline reagent comprises quaternary ammonium cations with alkoxysilyl groups, phosphonium groups, an alkyl group with a bulkier substituent or an alkoxyl group with a bulkier substituent. In certain embodiments the alkylammonium cations used in this regard function as a base rather than as a surfactant or template.

[0051] In certain embodiments using ammonia, ammonium hydroxide or alkali metal hydroxides, amorphous material is also present with the crystalline material in the product. In certain embodiments, upon calcining the as-made HOCMMs there is a reduction in the amount of apparent amorphous material present (for example an overall broad band at 25° (2θ) in XRD), indicative of apparent "self-healing" after calcination. In certain embodiments, by the controlled hydrolysis of urea to ammonium hydroxide there is a reduction in the amount of apparent amorphous material present in the HOCMMs (for example an overall broad band at 25° (2θ) in XRD), when compared with alternative routes such as NaOH or directly with ammonium hydroxide.

[0052] In the methods for synthesis of hierarchically ordered CMMs having well-defined long-range mesoporous ordering disclosed herein, suitable surfactants as supramolecular templates are provided to assist the reassembly and recrystallization of dissolved components (oligomers) by covalent and/or electrovalent interactions. Supramolecular templates are provided at a concentration in the aqueous suspension of about 0.01-0.5 M. In certain embodiments suitable supramolecular templates are provided at a concentration in the aqueous suspension of about 0.5-wt %. Suitable supramolecular templates are characterized by constrained diffusion within the micropore channels of parent CMM, referred to as bulky surfactants or bulky supramolecular templates. Diffusion of supramolecular template molecules into micropore-channels or cavities encourages CMM dissolution. This is minimized in the top-down methods for synthesis of hierarchically ordered CMMs having well-defined long-range mesoporous ordering disclosed herein, wherein effective supramolecular templates mini-

mize diffusion or partial diffusion thereof into CMM pore-channels, cavities or window openings. Such supramolecular templates possess suitable dimensions to block such diffusion. The suitable dimensions can be a based on dimensions of a head group and/or a tail group of a supramolecular template. In certain embodiments suitable dimensions can be based on a co-template having one or more components with suitable head and/or tail groups, or being a template system arranged in such a way, so as to minimize or block diffusion in to CMM pore-channels, cavities or window openings. By minimizing diffusion of templates into the CMM pore channels, CMM dissolution into oligomers and comprehensive reorganization and assembly into the hierarchically ordered CMMs having well-defined long-range mesoporous ordering disclosed herein is encouraged. In certain embodiments, a supramolecular template is one in which at least a substantial portion, a significant portion or a major portion of the surfactant does not enter into pores and/or channels of the CMM. For example, organosilanes (~0.7 nm) are relatively large compared to quaternary ammonium surfactants without such bulky groups including cetyltrimethylammonium bromide (CTAB) (~0.25 nm). In certain embodiments, a supramolecular template contains a long chain linear group (>~0.6 nm). In certain embodiments, a supramolecular template contains an aromatic or aromatic derivative group (>~0.6 nm). In certain embodiments, supramolecular templates contain one or more bulky groups having a dimension based on modeling of molecular dimensions as a cuboid having dimensions A, B and C, using Van der Waals radii for individual atoms, wherein one or more, two or more, or all three of the dimensions A, B and C are sufficiently close in dimension, or sufficiently larger in dimension, that constrains diffusion into the micropores of the selected parent CMM.

[0053] In certain embodiments an effective surfactant as a supramolecular template contains at least one moiety, as a head group or a tail group, selected from the group consisting of organosilanes, hydroxysilyls, alkoxysilyls, aromatics, branched alkyls, sulfonates, carboxylates, phosphates and combinations comprising one of the foregoing moieties. In certain embodiments an effective supramolecular template is an organosilane that contains at least one hydroxysilyl as a head group moiety. In certain embodiments an effective supramolecular template is an organosilane that contains at least one hydroxysilyl as a tail group moiety. In certain embodiments an effective supramolecular template is an organosilane that contains at least one alkoxysilyl as a head group moiety. In certain embodiments an effective supramolecular template is an organosilane that contains at least one alkoxysilyl as a tail group moiety. In certain embodiments an effective supramolecular template contains at least one aromatic as a head group moiety. In certain embodiments an effective supramolecular template contains at least one aromatic as a tail group moiety. In certain embodiments an effective supramolecular template contains at least one branched alkyl as a head group moiety. In certain embodiments an effective supramolecular template contains at least one branched alkyl as a tail group moiety. In certain embodiments an effective supramolecular template contains at least one sulfonate as a head group moiety. In certain embodiments an effective supramolecular template contains at least one sulfonate as a tail group moiety. In certain embodiments an effective supramolecular template contains at least one carboxylate as a head group moiety. In certain embodiments an effective supramolecular template contains at least one carboxylate as a tail group moiety. In certain embodiments an effective supramolecular template contains at least one phosphate as a head group moiety. In certain embodiments an effective supramolecular template contains at least one phosphate as a tail group moiety. These moieties are characterized by one or more dimensions that constrain diffusion into pores of a parent CMM. In certain embodiments, in which the CMM is characterized by pores of various dimensions, the selected moieties are characterized by one or more dimensions that constrain diffusion into the largest pores the parent CMM.

[0054] In certain embodiments an effective supramolecular template contains at least one cationic moiety. In certain embodiments an effective supramolecular template contains at least one cationic moiety selected from the group consisting of a quaternary ammonium moiety and a phosphonium moiety. In certain embodiments an effective supramolecular template contains at least one quaternary ammonium group having a terminal alkyl group with 6-24 carbon atoms. In certain embodiments an effective supramolecular template contains two quaternary ammonium groups wherein an alkyl group bridging the quaternary ammonium groups contains 1-10 carbon atoms. In certain embodiments an effective supramolecular template contains at least one quaternary ammonium group, and at least one constituent group, a head group moiety as described above. In certain embodiments an effective supramolecular template contains at least one quaternary ammonium group, and at least one constituent group, a tail group moiety as described above. In certain embodiments an effective supramolecular template contains at least one quaternary ammonium group, at least one constituent group, a head group moiety as described above, and an alkyl group that contains 1-10 carbon atoms bridging at least one of the quaternary ammonium groups and at least one of the head groups. In certain embodiments an effective supramolecular template contains at least one quaternary ammonium group, at least one constituent group, a tail group moiety as described above, and an alkyl group that contains 1-10 carbon atoms bridging at least one of the quaternary ammonium groups and at least one of the tail groups.

[0055] In certain embodiments an effective supramolecular template comprises a quaternary ammonium compound and a constituent group comprising one or more bulky organosilane or alkoxysilyl substituents. In certain embodiments an effective supramolecular template comprises a quaternary ammonium compound and a constituent group comprising one or more long-chain organosilane or alkoxysilyl substituents. In certain embodiments an effective supramolecular template cation comprises dimethyloctadecyl(3-trimethoxysilyl-propyl)-ammonium or derivatives of dimethyloctadecyl(3-trimethoxysilyl-propyl)-ammonium. In certain embodiments an effective supramolecular template cation comprises dimethylhexadecyl(3-trimethoxysilyl-propyl)-ammonium or derivatives of dimethylhexadecyl(3-trimethoxysilyl-propyl)-ammonium. In certain embodiments an effective supramolecular template cation comprises a double-acyloxy amphiphilic organosilane such as [2,3-bis(dodecanoyloxy)-propyl](3-(trimethoxy silyl)propyl)-dimethylammonium or derivatives of [2,3-bis(dodecanoyloxy)-propyl](3-(trimethoxysilyl)propyl)-dimethylammonium.

[0056] In certain embodiments an effective supramolecular template comprises a quaternary phosphonium com-

pound and a constituent group comprising one or more bulky aromatic substituents. In certain embodiments an effective supramolecular template comprises a quaternary phosphonium compound and a constituent group comprising one or more bulky alkoxysilyl or organosilane substituents.

[0057] In certain embodiments an effective supramolecular template contains a tail group moiety selected from the group consisting of aromatic groups containing 6-50, 6-25, 10-50 or 10-25 carbon atoms, alkyl groups containing 1-50, 1-25, 5-50, 5-25, 10-50 or 10-25 carbon atoms, aryl groups containing 1-50, 1-25, 5-50, 5-25, 10-50 or 10-25 carbon atoms, or a combination of aromatic and alkyl groups having up to 50 carbon atoms. In certain embodiments an effective supramolecular template contains a head group moiety selected from the group consisting of aromatic groups containing 6-50, 6-25, 10-50 or 10-25 carbon atoms, alkyl groups containing 1-1-25, 5-50, 5-25, 10-50 or 10-25 carbon atoms, aryl groups containing 1-50, 1-25, 5-50, 5-25, or 10-25 carbon atoms, or a combination of aromatic and alkyl groups having up to 50 carbon atoms. In certain embodiments an effective supramolecular template contains co-templated agents selected from the group consisting of quaternary ammonium compounds (including for example quaternary alkyl ammonium cationic species) and quaternary phosphonium compounds.

[0058] In certain embodiments effective supramolecular templates comprise (a) at least one of: aromatic quaternary ammonium compounds, branched alkyl chain quaternary ammonium compounds, alkyl benzene sulfonates, alkyl benzene phosphonates, alkyl benzene carboxylates, or substituted phosphonium cations; and (b1) and a constituent group comprising at least one of organosilanes, hydroxysilyls, alkoxysilyls, aromatics, branched alkyls, sulfonates, carboxylates or phosphates, as a head group; or (b2) and a constituent group comprising at least one of organosilanes, hydroxysilyls, alkoxysilyls, aromatics, branched alkyls, sulfonates, carboxylates or phosphates, as a tail group. In certain embodiments effective supramolecular templates include a sulfonate group (a non-limiting example is sulfonated bis(2-hydroxy-5-dodecylphenyl)methane (SBHDM)). In certain embodiments effective supramolecular templates include a carboxylate group (a non-limiting example is sodium 4-(octyloxy) benzoate). In certain embodiments effective supramolecular templates include a phosphonate group (a non-limiting example is tetradecyl(1, 4-benzene)bisphosphonate). In certain embodiments effective supramolecular templates include an aromatic group (a non-limiting example is benzylcetyldimethylammonium chloride). In certain embodiments effective supramolecular templates include an aliphatic group (a non-limiting example is tetraoctylammonium chloride).

[0059] The supramolecular template is provided as a cation/anion pair. In certain embodiments a cation of a supramolecular template is as described above is paired with an anion selected such as Cl^-, Br^-, OH^-, F^- and I^-. In certain embodiments a cation of a supramolecular template is as described above is paired with an anion such as Cl^-, Br^- or OH^-. In certain embodiments an effective supramolecular template comprises dimethyloctadecyl[3-(trimethoxysilyl) propyl]ammonium chloride (commonly abbreviated as "TPOAC") or derivatives of dimethyloctadecyl[3-(trimethoxysilyl)propyl]ammonium chloride. In certain embodiments an effective supramolecular template comprises dimethylhexadecyl[3-(trimethoxysilyl)propyl]ammonium chloride or derivatives of dimethylhexadecyl[3-(trimethoxysilyl)propyl]ammonium chloride. In certain embodiments an effective supramolecular template comprises [2,3-bis(dodecanoyloxy)-propyl](3-(trimethoxysilyl) propyl)-dimethylammonium iodide or derivatives of [2,3-bis(dodecanoyloxy)-propyl](3-(trimethoxysilyl)propyl)-dimethylammonium iodide.

[0060] In certain embodiments, the system includes an effective amount of an ionic co-solute (that is, in addition to the anion paired with the supramolecular template). In certain embodiments in which an ionic co-solute is used it is provided at a concentration in the aqueous suspension of about 0.01-0.5 M. In certain embodiments in which an ionic co-solute is used it is provided at a concentration in the aqueous suspension of about 0.01-5 wt %. In certain embodiments an ionic co-solute is selected from the group consisting of CO_3^{2-}, SO_4^{2-}, $SO_2O_3^{2-}$, $H_2PO_4^-$, F^-, Cl^-, Br^-, NO_3^-, I^-, ClO_4^-, SCN^- and $C_6H_5O_8^{-3}$ (citrate). In certain embodiments an ionic co-solute is selected from the group consisting of SO_4^{2-}, NO_3^-, and ClO_4^-. In certain embodiment an ionic co-solute is selected based on the Hofmeister series/Lyotropic series to control the curvature/shape of the micelles to yield the desired mesophase symmetry, for example, hexagonal, cubic or lamellar. In certain embodiments a nitrate (NO_3^-) is an ionic co-solute selected based on the Hofmeister series/Lyotropic series to control the curvature/shape of the micelles to yield hierarchically ordered CMMs having well-defined long-range mesoporous ordering possess a cubic mesophase symmetry; in certain embodiments using nitrate as an ionic co-solute, a nitrate salt is used, such as ammonium nitrate or a metal nitrate, wherein the metal can be an alkali metal, an alkali earth metal, a transition metal, a noble metal or a rare earth metal. In certain embodiments a sulfate (SO_4^{2-}) is an ionic co-solute selected based on the Hofmeister series/Lyotropic series to control the curvature/shape of the micelles to yield hierarchically ordered CMMs having well-defined long-range mesoporous ordering possess a hexagonal mesophase symmetry; in certain embodiments using sulfate as an ionic co-solute, a sulfate salt is used, such as ammonium sulfate or a metal sulfate, wherein the metal can be an alkali metal, an alkali earth metal, a transition metal, a noble metal or a rare earth metal. In certain embodiments a perchlorate (ClO_4^-) is an ionic co-solute selected based on the Hofmeister series/Lyotropic series to control the curvature/shape of the micelles to yield hierarchically ordered CMMs having well-defined long-range mesoporous ordering possess a lamellar mesophase symmetry; in certain embodiments using perchlorate as an ionic co-solute, a sulfate salt is used, such as sodium perchlorate, or another metal perchlorate, wherein the metal can be an alkali metal, an alkali earth metal, a transition metal, a noble metal or a rare earth metal.

[0061] The present disclosure is applicable to various types of CMMs as a parent material, including zeolite or zeolite-type materials. In certain embodiments a parent CMM exhibits both good crystallinity and Al-distribution to obtain high-quality HOCMMs while minimizing composite phases and/or impurities.

[0062] Suitable zeolitic materials as a parent CMM include those identified by the International Zeolite Association, including those with the identifiers ABW, ACO, AEI, AEL, AEN, AET, AFG, AFI, AFN, AFO, AFR, AFS, AFT, AFV, AFX, AFY, AHT, ANA, ANO, APC, APD, AST, ASV, ATN, ATO, ATS, ATT, ATV, AVE, AVL, AWO, AWW,

BCT, BEC, BIK, BOF, BOG, BOZ, BPH, BRE, BSV, CAN, CAS, CDO, CFI, CGF, CGS, CHA, -CHI, -CLO, CON, CSV, CZP, DAC, DDR, DFO, DFT, DOH, DON, EAB, EDI, EEI, EMT, EON, EPI, ERI, ESV, ETL, ETR, ETV, EUO, EWO, EWS, EZT, FAR, FAU, FER, FRA, GIS, GIU, GME, GON, GOO, HEU, IFO, IFR, -IFT, -IFU, IFW, IFY, IHW, IMF, IRN, IRR, —IRY, ISV, ITE, ITG, ITH, ITR, ITT, -ITV, ITW, IWR, IWS, IWV, IWW, JBW, JNT, JOZ, JRY, JSN, JSR, JST, JSW, KFI, LAU, LEV, LIO, -LIT, LOS, LOV, LTA, LTF, LTJ, LTL, LTN, MAR, MAZ, MEI, MEL, MEP, MER, MFI, MFS, MON, MOR, MOZ, MRT, MSE, MSO, MTF, MTN, MTT, MTW, MVY, MWF, MWW, NAB, NAT, NES, NON, NPO, NPT, NSI, OBW, OFF, OKO, OSI, OSO, OWE, -PAR, PAU, PCR, PHI, PON, POR, POS, PSI, PTO, PTT, PTY, PUN, PWN, PWO, PWW, RHO, -RON, RRO, RSN, RTE, RTH, RUT, RWR, RWY, SAF, SAO, SAS, SAT, SAV, SBE, SBN, SBS, SBT, SEW, SFE, SFF, SFG, SFH, SFN, SFO, SFS, SFW, SGT, SIV, SOD, SOF, SOR, SOS, SOV, SSF, SSY, STF, STI, STT, STW, -SVR, SVV, SWY, -SYT, SZR, TER, THO, TOL, TON, TSC, TUN, UEI, UFI, UOS, UOV, UOZ, USI, UTL, UWY, VET, VFI, VNI, VSV, WEI, -WEN, YFI, YUG, ZON, *BEA, *CTH, *-EWT, *-ITN, *MRE, *PCS, *SFV, *-SSO, *STO, *-SVY and *UOE. For example, certain zeolites known to be useful in the petroleum refining industry include but are not limited to AEI, *BEA, CHA, FAU, MFI, MOR, LTL, LTA or MWW. In certain embodiments a parent zeolite can be (FAU) framework zeolite, which includes USY, for example having a micropore size related to the 12-member ring when viewed along the [111] direction of 7.4×7.4 Å. In certain embodiments a parent zeolite can be (MFI) framework zeolite, which includes ZSM-5, for example having a micropore size related to the 10-member rings when viewed along the [100] and [010] directions of 5.5×5.1 Å and 5.6×5.3 Å, respectively. In certain embodiments a parent zeolite can be (MOR) framework zeolite, which includes mordenite zeolites, for example having a micropore size related to the 12-member ring and 8-member ring when viewed along the [001] and [001] directions of 6.5×7.0 Å and 2.6×5.7 Å, respectively. In certain embodiments a parent zeolite can be (*BEA) framework zeolite, which includes zeolite beta polymorph A, for example having a micropore size related to the 12-member rings when viewed along the [001] and [001] directions of 6.6×6.7 Å and 5.6×5.6 Å, respectively. In certain embodiments a parent zeolite can be (CHA) framework zeolite, which includes chabazite zeolite, for example having a micropore size related to the 8-member ring when viewed normal to the [001] direction of 3.8×3.8 Å. In certain embodiments a parent zeolite can be (LTL) framework zeolite, which includes Linde Type L zeolite (zeolite L), for example having a micropore size related to the 12-member ring when viewed along the [001] direction of 7.1×7.1 Å. In certain embodiments a parent zeolite can be (LTA) framework zeolite, which includes Linde Type A zeolite (zeolite A), for example having a micropore size related to the 8-member ring when viewed along the [100] direction of 4.1×4.1 Å. In certain embodiments a parent zeolite can be (AEI) framework zeolite, for example having a micropore size related to the 8-member ring when viewed normal to the [001] direction of 3.8×3.8 Å. In certain embodiments a parent zeolite can be (MWW) framework zeolite, which includes MCM-22, for example having a micropore size related to the 10-member rings when viewed normal to direction 'between layers' and 'within layers' of 4.0×5.5 Å and 4.1×5.1 Å, respectively.

[0063] In certain embodiments a parent CMM is a zeolite-type material, for example, aluminophosphates (AlPO), silicon-substituted aluminophosphates (SAPO), or metal-containing aluminophosphates (MAPO). In certain embodiments a parent CMM is a zeolitic siliceous only framework material.

[0064] As described above, embodiments herein include supramolecular templates that contain one or more bulky groups having a dimension based on modeling of molecular dimensions as a cuboid having dimensions A, B and C, using Van der Waals radii for individual atoms, wherein one or more, two or more, or all three of the dimensions A, B and C are sufficiently close in dimension, or sufficiently larger in dimension, that constrains diffusion into the micropores of the CMM. Also as described above with respect to the known parameters related to pore dimensions for exemplary zeolites, such parameters influence the selection of a supramolecular template. For instance, in the examples herein, FAU zeolite is used; when the supramolecular template material was CTAB (~0.25 nm), HOCMMs were not realized; however, when the supramolecular template was an organosilane (~0.7 nm), HOCMMs were realized, as these are closer in dimension to the pore dimensions for FAU zeolite and therefore are constrained from entering such pores. Likewise, suitable supramolecular templates are determined based on a selected parent CMM.

[0065] In certain embodiments parent CMMs used in the methods are zeolites herein having a SAR suitable for the particular type of zeolite. In general, the SAR of parent zeolites can be in the range of about 2-10000, 2-5000, 2-500, 2-100, 2-80, 5-10000, 5-5000, 5-500, 5-100, 5-80, 10-10000, 10-5000, 10-500, 10-100, 10-80, 50-10000, 50-5000, 50-1000, 50-500 or 50-100. In certain embodiments the SAR of the parent zeolite is greater than or equal to 5 or 10 to achieve long-range ordering. In embodiments with a SAR of less than 10, uniform mesoporosity and certain degree of ordering is attainable, and amorphous framework material remains in the product.

Synthesis Steps

[0066] FIGS. **1** and **2** are schematic overviews of the hierarchical ordering by post-synthetic ensembles synthesis route described herein, including the general synthesis mechanism of and how AHE influences g values to alter the micellar curvature and induce mesophase transition. Although the CMM schematically depicted in FIGS. **1** and **2** is FAU zeolite, it is appreciated that other CMMs can be utilized as a parent CMM by post-synthetic ensembles synthesis route.

[0067] The method includes base-mediated dissolution/incision of parent CMMs into oligomeric components, and reorganization into hierarchically ordered mesostructures by supramolecular templating, and in certain embodiments by the Hofmeister effect. The parent CMM **10** is provided in crystalline form. An effective amount of an alkaline reagent and an effective amount of a surfactant for supramolecular templating are added to form an aqueous suspension, and that suspension is maintained under hydrothermal conditions to form oligomeric CMM units **12** of the parent CMM (such as oligomeric zeolitic units when the parent CMM is zeolite). The supramolecular template molecules **14** form

into shaped micelles **16** (not shown in FIG. **2**) and oligomeric CMM units hierarchically reassemble and crystallize around the shaped micelles as an ordered mesostructure, HOCMM **18**, having mesopores **20** of defined symmetry and mesopore walls formed of the oligomeric CMM units thereby retaining micropores **22** of the underlying CMM structure of the parent CMM. In certain embodiments, a composition of matter produced by the method herein is the HOCMM **18** that contains shaped micelles **16**. In certain embodiments, a composition of matter produced herein is the HOCMM **18** having the surfactant **14** formed into shaped micelles **16** removed, for example by: chemical methods such as solvent extraction, chemical oxidation, or ionic liquid treatment; or physical methods such as calcination, supercritical CO_2, microwave-assisted treatment, ultrasonic-assisted treatment, ozone treatment, or plasma technology.

[0068] Distinctive mesophase transitions of hierarchical ensembles to yield distinct mesostructures can be attributed to the synergetic action of the anionic Hofmeister effect (ion-specific interactions) in supramolecular self-assembly. Anions of different sizes and charges possess different polarizabilities, charge densities, and hydration energies in aqueous solutions. When paired with a positive surfactant head group, these properties can affect the electrostatic repulsions among the head groups and hydration at the micellar interface, thus changing the area of the head group (a_0). Such short-range ion-specific interactions can be a significant driving force in changing the micellar curvature and inducing mesophase transition.

[0069] Referring to FIG. **2**, the general synthesis mechanism is shown including a schematic representation of how AHE influences g values to alter the micellar curvature and induce mesophase transition. The surfactant (also referred to herein as the supramolecular template) to co-solute molar ratio (which may be expressed as a surfactant to salt molar ratio) is effective to produce the desired mesoporous structure. The surfactant to co-solute molar ratio is selected to result in surfactant packing parameters suitable to induce the mesophase transitions to the desired geometry inducing changes to the curvature of the micelles. For example, when a sulfate is used as an ionic co-solute, the micellar curvature is represented by a surfactant packing parameter g of about ½, or about 0.4-0.6, or 0.5, and the resulting HOCMM possesses long-range mesoporous ordering of hexagonal symmetry. When a nitrate is used as an ionic co-solute, the micellar curvature is represented by a surfactant packing parameter g in the range of about ½ to about 2/3, or about 0.4-0.8, 0.4-0.67, 0.5-0.8 or 0.5-0.67, and the resulting HOCMM possesses long-range mesoporous ordering of cubic symmetry. When a perchlorate is used as an ionic co-solute, the micellar curvature is represented by a surfactant packing parameter g in the range of about 0.9-1.1 or 1, and the resulting HOCMM possesses long-range mesoporous ordering of lamellar symmetry. For example, in certain embodiments a surfactant to co-solute molar ratio for synthesis of HOCMM possessing long-range mesoporous ordering of hexagonal symmetry may be in the range of about 0.8-1.3, 0.9-1.3, 0.9-12 or 0.8-1.2. For example, in certain embodiments a surfactant to co-solute molar ratio for synthesis of HOCMM possessing long-range mesoporous ordering of cubic symmetry may be in the range of about 0.8-1.3, 0.9-1.3, 0.9-12 or 0.8-1.2. For example, in certain embodiments a surfactant to co-solute molar ratio for synthesis of HOCMM possessing long-range mesoporous ordering of lamellar symmetry may be in the range of about 0.2-0.7, 0.3-0.2-0.6 or 0.3-0.6. It is appreciated that wider ranges may be applicable, as recited herein, and that these ranges may vary depending on the selected surfactant and co-solutes that influence the values of V (total volume of surfactant tails), a_0 (area of the head group) and 1 (length of surfactant tail) to determine g (surfactant packing parameter). In certain embodiments, the ranges of surfactant packing parameter g and/or the ranges of surfactant to co-solute molar ratio are effective for an organosilane supramolecular template, for example, dimethyloctadecyl(3-trimethoxysilyl-propyl)-ammonium or a derivative of dimethyloctadecyl(3-trimethoxysilyl-propyl)-ammonium.

[0070] FIG. **2** also shows the influence of ion-specific interactions (The Hofmeister effect) on the micellar curvature in a self-assembly process. Anions of different sizes and charges possess different polarizabilities, charge densities and hydration energies in aqueous solutions. When paired with a positive surfactant head group, these properties can affect the electrostatic repulsions among the head groups and hydration at the micellar interface, thus changing the area of the head group (a_0). Such short-range ion-specific interactions can be a significant driving force in changing the micellar curvature and inducing mesophase transition. Based on the Hofmeister series (SO_4^{2-}>HPO_4^{2-}>Oac^->Cl^->Br^->NO_3^->ClO_4^->SCN^-), the strongly hydrated ions (left side of series) can increase the micellar curvature, whereas weakly hydrated ions can decrease the micellar curvature. While not wishing to be bound by theory, influence of co-solutes such as salts in mesophase ordering can be attributed to their charge-balancing effect; in the surfactant self-assembly, a high density of surfactant molecules is closely packed into micelles due to the hydrophobic effect; as a result, electrostatic repulsions of the charged head group should be minimized by the counter anions to induce facile aggregation; as such auxiliary counteranions play a role in stabilizing the micelles despite the gradual changes in the concentration of polyanionic zeolite components.

[0071] An effective amount of a solvent is used in the process. In certain embodiments the solvent is water. In certain embodiments the solvent is water in the presence of co-solvents selected from the group consisting of polar solvents, non-polar solvents and pore swelling agents (such as 1,3,5-trimethylbenzene). In certain embodiments the solvent selected from the group consisting of polar solvents, non-polar solvents and pore swelling agents (such as 1,3,5-trimethylbenzene), in the absence of water. In an embodiment, mixture components are added with water to the reaction vessel prior to heating. Typically, water allows for adequate mixing to realize a more homogeneous distribution of the suspension components, which ultimately produces a more desirable product because each crystal is more closely matched in properties to the next crystal. Insufficient mixing could result in undesirable products with respect to amorphous phases or a lesser degree of long-range order.

[0072] The suspension components are combined in any suitable sequence and are sufficiently mixed to form a homogeneous distribution of the suspension components. The suspension can be maintained in an autoclave under autogenous pressure (from the components or from the components plus an addition of a gas purge into the vessel prior to heating), or in another suitable vessel, under agita-

tion such as by stirring, tumbling and/or shaking. Mixing of the suspension components is conducted between about 20-60, 20-50 or 20-40° C.

[0073] The steps of incision and reassembly occur during hydrothermal treatment to form a solid (product, HOCMM having well-defined long-range mesoporous ordering) suspended in a supernatant (mother liquor). Hydrothermal treatment is conducted: for a period of about 4-168, 12-168, 24-168, 4-96, 12-96 or 24-96 hours; at a temperature of about 70-250, 70-210, 70-180, 70-150, 90-250, 90-210, 90-180, 90-160, 90-150, 110-250, 110-210, 110-180, 110-160, or 110-150° C.; and at a pressure of about atmospheric to autogenous pressure. In certain embodiments hydrothermal treatment occurs in a vessel that is the same as that used for mixing, or the suspension is transferred to another vessel (such as another autoclave or low-pressure vessel). In certain embodiments the vessel used for hydrothermal treatment is static. In certain embodiments the vessel used for hydrothermal treatment is under agitation that is sufficient to suspend the components.

[0074] The HOCMM having well-defined long-range mesoporous ordering is the product recovered. The solids are recovered using known techniques such as centrifugation, decanting, gravity, vacuum filtration, filter press, or rotary drums. The recovered HOCMM having well-defined long-range mesoporous ordering is dried, for example at a temperature of about 50-150, 80-150 or 80-120° C., at atmospheric pressure or under vacuum conditions, for a time of about 0.5-96, 12-96 or 24-96 hours.

[0075] In certain embodiments, the dried HOCMM having well-defined long-range mesoporous ordering is calcined, for example to remove supramolecular templates that remain in the mesopores and other constituents from the mesopores and/or the discrete zeolite cell micropores. The conditions for calcination in embodiments in which it is carried out can include temperatures in the range of about 350-650, 350-600, 350-550, 500-650, 500-600 or 500-550° C., atmospheric pressure or under vacuum, and a time period of about 2.5-24, 2.5-12, 5-24 or 5-12 hours. Calcining can occur with ramp rates in the range of from about 0.1-10, 0.1-5, 0.1-3, 1-10, 1-5 or 1-3° C. per minute. In certain embodiments calcination can have a first step ramping to a temperature of between about 100-150° C. with a holding time of from about 1.5-6 or 1-12 hours (at ramp rates of from about 0.1-5, 0.1-3, 1-5 or 1-3° C. per min) before increasing to a higher temperature with a final holding time in the range of about 1.5-6 or 1-12 hours.

[0076] In certain embodiments, the supernatant remaining after recovery of product from the system is recovered, and all or a portion thereof can be reused as all or a portion of the solution in a subsequent process for synthesis of HOCMM having well-defined long-range mesoporous ordering. In this embodiment, recovered supernatant used in subsequent process is referred to as supernatant from a prior synthesis. In certain embodiments a new synthesis can occur using supernatant from a prior synthesis together with parent CMM. In certain embodiments a new synthesis can occur using supernatant from a prior synthesis together with parent CMM and an additional quantity of make-up alkaline reagent (for example urea). In certain embodiments a new synthesis can occur using supernatant from a prior synthesis together with parent CMM and an additional quantity of make-up supramolecular template. In certain embodiments a new synthesis can occur using supernatant from a prior synthesis together with parent CMM and an additional quantity of make-up ionic co-solute. In certain embodiments a new synthesis can occur using supernatant from a prior synthesis together with parent CMM and an additional quantity of make-up alkaline reagent (for example urea) and/or make-up supramolecular template and/or optional make-up ionic co-solute.

Products

[0077] The composition of matter recovered as described herein are hierarchically ordered CMMs (such as zeolites) having well-defined long-range mesoporous ordering. These are characterized by defined mesoporous channel directions with zeolite micropore channels in the walls of the mesostructure. The HOCMM having well-defined long-range mesoporous ordering recovered from synthesis possesses supramolecular template as described herein in the mesopores (that is, prior to calcination or extraction of the supramolecular template). In certain embodiments the HOCMM having well-defined long-range mesoporous ordering recovered from synthesis possesses micelles of supramolecular template as described herein in the mesopores (that is, prior to calcination or extraction of the supramolecular template). The composition of matter recovered as described herein retains the structural integrity of the microporous zeolite structure by controlled incision of the parent zeolite followed by controlled reassembly of the zeolite oligomers under a controlled micellar curvature to yield the HOCMMs with defined mesoporous symmetry.

[0078] This well-defined long-range mesoporosity is elusive in the field of hierarchically ordered zeolites. The long-range order is defined by secondary peaks associated with the periodic arrangement of mesopores in x-ray diffraction (XRD) patterns for the given mesophase, and/or by observations in microscopy, as demonstrated in the examples herein. These peaks associated with the mesoporous traits of the products are observed at low 20 angles. The material also exhibits high-angle peaks associated with the zeolites and are observed at high 2-theta angles. In certain embodiments the low-angle peaks refer to those occurring at 20 angles less than about 6°.

[0079] In certain embodiments herein, long-range mesoporous ordering of HOCMMs produced according to the methods described herein are characterized by the mesopore periodicity repeating over a length of greater than about 50 nm.

[0080] In certain embodiments herein, HOCMMs produced according to the methods described herein are cubic mesophase possessing Ia-3d symmetry and long-range mesoporous ordering is characterized by secondary XRD peaks associated with the periodic arrangement of mesopores are present at one or more of the (220), (321), (400), (420) and (332) reflections. In certain embodiments herein, HOCMMs produced according to the methods described herein are hexagonal mesophase possessing p6 mm symmetry and long-range mesoporous ordering is characterized by secondary peaks in XRD that are present at (11) and/or (20) reflections. In certain embodiments herein, HOCMMs produced according to the methods described herein are lamellar mesophase possessing p2 symmetry and long-range mesoporous ordering is characterized by secondary peaks in XRD that are present at a (200) reflection.

[0081] In certain embodiments herein, HOCMMs having well-defined long-range mesoporous ordering produced

according to the methods described herein possess a surface area of about 200-1500, 200-1000, 200-900, 400-1500, 400-1000, 400-900, 500-1500, 500-1000 or 500-900 m 2/g. In embodiments herein, the HOCMMs having well-defined long-range mesoporous ordering produced according to the methods described herein possess mesoporous pore size of about 2-50, 2-20 or 2-10 nm. In embodiments herein, the HOCMMs having well-defined long-range mesoporous ordering produced according to the methods described herein possess a silica-to-alumina ratio of about 2.5-1500, 3-1500, 4-1500, 5-1500, 6-1500, 2.5-1000, 3-1000, 4-1000, 5-1000, 6-1000, 2.5-500, 3-500, 4-500, 5-500, 6-500, 2.5-100, 3-100, 4-100, 5-100, or 6-100. In embodiments herein, the HOCMMs having well-defined long-range mesoporous ordering produced according to the methods described herein possess a total pore volume of about 0.01-1.50, 0.01-1.0, 0.01-0.75, 0.01-0.65, 0.1-1.50, 0.1-1.0, 0.1-0.75, 0.1-0.65, 0.2-1.50, 0.2-1.0, 0.2-0.2-0.65, 0.3-1.50, 0.3-1.0, 0.3-0.75 or 0.3-0.65 cc/g.

[0082] In embodiments herein, a product produced by the above method and demonstrated in an example herein is characterized by a mesophase having cubic symmetry. In certain embodiments the product is a 3D-cubic ordered mesoporous zeolite. HOCMMs with the mesophase having cubic symmetry are characterized by cubic mesoporous channel directions with CMM micropore channels in the walls of the mesostructure. The cubic mesophase can possess one of 1a-3d, Fm-3m, Pm-3n, Pn-3m or Im-3m symmetry. In embodiments herein the cubic mesophase possesses 1a-3d symmetry and the secondary XRD peaks associated with the periodic arrangement of mesopores are present at one or more of the (220), (321), (400), (420) and (332) reflections. In embodiments herein the cubic mesophase possesses 1a-3d symmetry and the high-degree of long-range cubic mesophase ordering is observable by microscopy viewed by the electron beam down a suitable zone axis, for example the [311], or zone axes. In the example herein, nitrate salt (NO_3^-) is used as an ionic co-solute is used to generate the mesophase having cubic symmetry. In these embodiments CMM structures are arranged in a cubic symmetry on the meso-scale, where the CMM particles (regardless of their atomic-level symmetry or structure) are arranged around micelles (on the meso-scale), and whereby the micelles are arranged exhibiting cubic symmetry. Accordingly, HOCMM having a cubic mesophase includes CMM characterized by atomic-level symmetry and possessing micropores that are inherent to that type of CMM, arranged in a cubic symmetry at the meso-scale level with mesopores, wherein walls of the mesopores and a mass of the mesostructure between mesopores is characterized by said CMM (e.g., crystalline zeolite). This is created as described herein by forming oligomers of the underlying CMM and arranging those oligomers arranged around micelles exhibiting cubic symmetry on the meso-scale. In one embodiment a HOCMM is provided including MFI zeolite having atomic-level orthorhombic symmetry arranged in a cubic symmetry meso-scale, wherein during synthesis of hierarchically ordered zeolite from parent MFI zeolite, oligomers of the parent MFI zeolite are formed and arranged around micelles exhibiting cubic symmetry on the meso-scale. In one embodiment a HOCMM is provided including CHA zeolite having atomic-level trigonal symmetry arranged in a cubic symmetry meso-scale, wherein during synthesis of hierarchically ordered zeolite from parent CHA zeolite, oligomers of the parent CHA zeolite are formed and arranged around micelles exhibiting cubic symmetry on the meso-scale. In one embodiment a HOCMM is provided including BEA zeolite having atomic-level tetragonal symmetry arranged in a cubic symmetry meso-scale, wherein during synthesis of hierarchically ordered zeolite from parent BEA zeolite, oligomers of the parent BEA zeolite are formed and arranged around micelles exhibiting cubic symmetry on the meso-scale. In one embodiment a HOCMM is provided including MWW zeolite having atomic-level hexagonal symmetry arranged in a cubic symmetry meso-scale, wherein during synthesis of hierarchically ordered zeolite from parent MWW zeolite, oligomers of the parent MWW zeolite are formed and arranged around micelles exhibiting cubic symmetry on the meso-scale. In one embodiment a HOCMM is provided including FAU zeolite having atomic-level cubic symmetry arranged in a cubic symmetry meso-scale, wherein during synthesis of hierarchically ordered zeolite from parent FAU zeolite, oligomers of the parent FAU zeolite are formed and arranged around micelles exhibiting cubic symmetry on the meso-scale.

[0083] In embodiments herein, a product produced by the above method and demonstrated in an example herein is characterized by a mesophase having hexagonal symmetry. In certain embodiments the product is a 2D-hexagonally ordered mesoporous zeolite. HOCMMs with the mesophase having hexagonal symmetry are characterized by hexagonal mesoporous channel directions with CMM micropore channels in the walls of the mesostructure. The hexagonal mesophase can possess one of p6m, p6 mm or p63/mmc symmetry. In embodiments herein the hexagonal mesophase possesses p6 mm symmetry and secondary XRD peaks associated with the periodic arrangement of mesopores are present at one or more of the (11) and (20) reflections. In embodiments herein the hexagonal mesophase possesses p6 mm symmetry and secondary XRD peaks are present at both the (11) and (20) reflections. In embodiments herein the hexagonal mesophase possesses p6 mm symmetry and the high-degree of long-range hexagonal p6 mm mesophase ordering is observable by microscopy viewed by the electron beam perpendicular to the pores down the zone axis and/or parallel to the pores down the zone axis. In these embodiments CMM structures are arranged in a hexagonal p6 mm symmetry on the meso-scale, where the CMM particles (regardless of their atomic-level symmetry or structure) are arranged around micelles (on the meso-scale), and whereby the micelles are arranged exhibiting hexagonal symmetry. Accordingly, HOCMM having a hexagonal p6 mm mesophase includes CMM characterized by atomic-level symmetry and possessing micropores that are inherent to that type of CMM, arranged in a hexagonal p6 mm symmetry at the meso-scale level with mesopores, wherein walls of the mesopores and a mass of the mesostructure between mesopores is characterized by said CMM (e.g., crystalline zeolite). This is created as described herein by forming oligomers of the underlying CMM and arranging those oligomers arranged around micelles exhibiting hexagonal symmetry on the meso-scale. In one embodiment a HOCMM is provided including MFI zeolite having atomic-level orthorhombic symmetry arranged in a hexagonal p6 mm symmetry meso-scale, wherein during synthesis of hierarchically ordered zeolite from parent MFI zeolite, oligomers of the parent MFI zeolite are formed and arranged

around micelles exhibiting hexagonal symmetry on the meso-scale. In one embodiment a HOCMM is provided including CHA zeolite having atomic-level trigonal symmetry arranged in a hexagonal p6 mm symmetry meso-scale, wherein during synthesis of hierarchically ordered zeolite from parent CHA zeolite, oligomers of the parent CHA zeolite are formed and arranged around micelles exhibiting hexagonal symmetry on the meso-scale. In one embodiment a HOCMM is provided including BEA zeolite having atomic-level tetragonal symmetry arranged in a hexagonal p6 mm symmetry meso-scale, wherein during synthesis of hierarchically ordered zeolite from parent BEA zeolite, oligomers of the parent BEA zeolite are formed and arranged around micelles exhibiting hexagonal symmetry on the meso-scale. In one embodiment a HOCMM is provided including MWW zeolite having atomic-level hexagonal symmetry arranged in a hexagonal p6 mm symmetry meso-scale, wherein during synthesis of hierarchically ordered zeolite from parent MWW zeolite, oligomers of the parent MWW zeolite are formed and arranged around micelles exhibiting hexagonal symmetry on the meso-scale. In one embodiment a HOCMM is provided including FAU zeolite having atomic-level cubic symmetry arranged in a hexagonal p6 mm symmetry meso-scale, wherein during synthesis of hierarchically ordered zeolite from parent FAU zeolite, oligomers of the parent FAU zeolite are formed and arranged around micelles exhibiting hexagonal symmetry on the meso-scale.

[0084] In embodiments herein, a product produced by the above method and demonstrated in an example herein is characterized by a high-degree of long-range lamellar mesophase ordering. In certain embodiments the product is a mesoporous zeolite of lamellar mesophase ordering. HOCMMs with the mesophase having lamellar symmetry are characterized by lamellar mesoporous channel directions with CMM micropore channels in the walls of the meso-structure. In these embodiments CMM structures are arranged in a lamellar symmetry on the meso-scale, where the CMM particles (regardless of their atomic-level symmetry or structure) are arranged around micelles (on the meso-scale), and whereby the micelles are arranged exhibiting lamellar symmetry. In certain embodiments lamellar symmetry is p2, p1 or pm symmetry. In certain embodiments lamellar symmetry is p2 symmetry with a secondary XRD peak associated with the periodic arrangement of mesopores present at least at the (200) reflection. In certain embodiments the high-degree of long-range lamellar mesophase ordering is observable by microscopy viewed by the electron beam in parallel or perpendicular directions to the zone axis. Accordingly, HOCMM having a lamellar mesophase includes CMM characterized by atomic-level symmetry and possessing micropores that are inherent to that type of CMM, arranged in a lamellar symmetry at the meso-scale level with mesopores, wherein walls of the mesopores and a mass of the mesostructure between mesopores is characterized by said CMM. This is created as described herein by forming oligomers of the underlying CMM and arranging those oligomers arranged around micelles exhibiting lamellar symmetry on the meso-scale. In one embodiment a HOCMM is provided including MFI zeolite having atomic-level orthorhombic symmetry arranged in a lamellar symmetry meso-scale, wherein during synthesis of hierarchically ordered zeolite from parent MFI zeolite, oligomers of the parent MFI zeolite are formed and arranged around micelles exhibiting lamellar symmetry on the meso-scale. In one embodiment a HOCMM is provided including CHA zeolite having atomic-level trigonal symmetry arranged in a lamellar symmetry meso-scale, wherein during synthesis of hierarchically ordered zeolite from parent CHA zeolite, oligomers of the parent CHA zeolite are formed and arranged around micelles exhibiting lamellar symmetry on the meso-scale. In one embodiment a HOCMM is provided including BEA zeolite having atomic-level tetragonal symmetry arranged in a lamellar symmetry meso-scale, wherein during synthesis of hierarchically ordered zeolite from parent BEA zeolite, oligomers of the parent BEA zeolite are formed and arranged around micelles exhibiting lamellar symmetry on the meso-scale. In one embodiment a HOCMM is provided including MWW zeolite having atomic-level hexagonal symmetry arranged in a lamellar symmetry meso-scale, wherein during synthesis of hierarchically ordered zeolite from parent MWW zeolite, oligomers of the parent MWW zeolite are formed and arranged around micelles exhibiting lamellar symmetry on the meso-scale. In one embodiment a HOCMM is provided including FAU zeolite having atomic-level cubic symmetry arranged in a lamellar symmetry meso-scale, wherein during synthesis of hierarchically ordered zeolite from parent FAU zeolite, oligomers of the parent FAU zeolite are formed and arranged around micelles exhibiting lamellar symmetry on the meso-scale.

[0085] In embodiments which CMM structures are arranged in a lamellar symmetry on the meso-scale, lamellar symmetry is primarily observed in the as-made materials (that is, prior to calcination). In the absence of CMM interconnections between lamellar structures, there is a tendency to collapse during calcination. In certain embodiments, CMMs such as zeolite crystalline structures arranged in a lamellar symmetry provided herein can be exfoliated to form sheets of the CMMs, for example zeolitic nanosheets. In certain embodiments, CMMs such as zeolite crystalline structures arranged in a lamellar symmetry provided herein can retain a lamellar symmetry by using pillaring techniques known in the art, for example wherein a silica source such as tetraethyl orthosilicate (TEOS) is condensed amidst the lamellar structures and crystallized during calcination to retain lamellar structure and prevent collapse (see, for example, Na, K. et al. "Pillared MFI Zeolite Nanosheets of a Single-unit-cell Thickness." *J. Am. Chem. Soc.* 132, 4169-4177. In embodiments in which the HOCMMs formed herein possess meso-scale, lamellar symmetry with a pillared lamellar structure, they can be used, for example, as a catalytic material or catalytic support material.

[0086] HOCMMs produced according to the present disclosure are effective as catalysts, or components of catalysts, in hydrocracking of hydrocarbon oil. The HOCMM can be used as a support having loaded thereon one or more active metal components as a hydrocracking catalyst. The active metal components are loaded, for example, carried on surfaces including the mesopore wall surfaces, micropore wall surfaces or mesopore and micropore wall surfaces; the active metal components are loaded according to known methods, such as providing an aqueous solution of the active metal components and subjecting HOCMM as catalyst support material to immersion, incipient wetness, and evaporative, or any other suitable method. In certain embodiments, the CMM of the HOCMM comprises zeolite. In certain embodiments the CMM of the HOCMM comprises

one or more zeolite types AEI, *BEA, CHA, FAU, MFI, MOR, LTL, LTA or MWW. In certain embodiments the CMM of the HOCMM comprises FAU zeolite.

[0087] The content of the HOCMM and the active metal component are appropriately determined according to the object. In certain embodiments, a hydrocracking catalyst comprises as a support the HOCMM and an inorganic oxide component, typically as a binder and/or granulating agent. For example, support particles (prior to loading of one or more hydrocracking active metal components) can contain HOCMM in the range of about 0.1-99, 0.1-90, 0.1-80, 0.1-70, 0.1-50, 2-99, 2-90, 2-80, 2-70, 2-50, 2-40, 20-100, 20-90, 20-80, 20-70, 20-50, or 20-40 wt %, with the remaining content being the inorganic oxide. In certain embodiments, support particles (prior to loading of one or more hydrocracking active metal components) can contain HOCMM in the range of about 0.1-99, 0.1-90, 0.1-80, 0.1-70, 0.1-50, 0.1-40, 2-99, 2-90, 2-80, 2-70, 2-50, 2-40, 20-90, 20-80, 20-70, 20-50, or 20-40 wt %, with the remaining content being the inorganic oxide and one or more other zeolitic materials.

[0088] As the inorganic oxide component, any material used in hydrocracking or other catalyst compositions in the related art can be used. Examples thereof include alumina, silica, titania, silica-alumina, alumina-titania, alumina-zirconia, alumina-boria, phosphorus-alumina, silica-alumina-boria, phosphorus-alumina-boria, phosphorus-alumina-silica, silica-alumina-titania, silica-alumina-zirconia, alumina-zirconia-titania, phosphorous-alumina-zirconia, alumina-zirconia-titania and phosphorus-alumina-titania.

[0089] The active metal component can include one or more metals or metal compounds (oxides or sulfides) known in the art of hydrocracking, including those selected from the Periodic Table of the Elements IUPAC Groups 6, 7, 8, 9 and 10. In certain embodiments the active metal component is one or more of Mo, W, Co or Ni (oxides or sulfides). The additional active metal component may be contained in catalyst in effective concentrations. For example, total active component content in hydrocracking catalysts can be present in an amount as is known in the related art, for example about 0.01-40, 0.1-40, 1-40, 2-40, 5-40, 0.01-30, 0.1-30, 1-30, 2-30, 5-30, 0.01-20, 0.1-1-20, 2-20 or 5-20 W % in terms of metal, oxide or sulfide. In certain embodiments, active metal components are loaded using a solution of oxides, and prior to use, the hydrocracking catalysts are sulfided.

EXAMPLES

[0090] The HOCMMs produced in the examples herein exhibit a remarkable degree of well-defined long-range mesoporous ordering, as given by the low-angle XRD patterns. Structural and textural properties of certain samples are provided in Table 3. The parent zeolite used in the examples and comparative examples possesses the FAU framework, zeolite Y (obtained from Zeolyst International, product name CBV 720) and is referred to herein as zeolite HY-15, having a SAR of about 30 (Si/Al atomic ratio of 15). While the examples are shown with respect to this particular zeolite, the methods herein can be applied to a parent CMM from another source and of another type as described herein, whether obtained from a commercial manufacturer obtained from a separate synthesis process. Accordingly, the resulting compositions of matter have the mesoporous structure with microporosity and CMM structure corresponding to the parent CMM. The solutions were prepared at room temperature (RT) and under stirring at 500 RPM.

[0091] Characterizations herein were carried out as follows. Powder x-ray diffraction patterns were obtained using a Bruker D8 twin diffractometer, operating at 40 kV and 40 mA having Cu Kα radiation (λ=0.154 nm) and a step-size of 0.02. N_2 physisorption measurements were conducted at 77 K using a Micromeritics ASAP 2420 instrument. All samples were degassed at 350° C. for 12 h before the analysis. The specific surface areas and pore size distributions were calculated using the Brunauer-Emmett-Teller (BET) and non-local density functional theory (NLDFT) models. The t-plot method was used to calculate the micropore volume. High-resolution transmission electron microscopy (TEM) studies were undertaken using a FEI-Titan ST electron microscope operated at 300 kV. Scanning electron microscopy (SEM) images were obtained with Nova Nano HR-SEM 240 microscope operated at 4 kV. The samples were sputter-coated with Platinum (Pt) prior to the analysis to eliminate the charge effect. The Si/Al ratios were calculated by solid-state magic-angle spinning nuclear magnetic resonance (MAS-NMR) experiments using a Bruker Advance 400 MHz instrument, applying 4 μs radio frequency pulses and a recycle delay of 60 s. Conversely, the bulk Si/Al ratios of the zeolites were calculated from the inductively coupled plasma-optical emission spectroscopy (ICP-OES) analysis performed using 5100 ICP-OES Agilent instruments. Prior to the analysis, the samples were mixed with hydrofluoric acid (HF) and nitric acid (HNO_3) and digested at 260° C. and 160 bar using an UltraWAVE microwave digestion system (Milestone).

[0092] For the acquisition of the electron micrographs for tomography reconstruction, the zeolite powder was deposited on a Quantifoil 300 mesh TEM grid supporting a 2 nm thick continuous carbon film over a holey carbon membrane. Prior to the zeolite deposition, a diluted solution of gold nanoparticles (AuNPs) around 5 nm in diameter was dispersed on the TEM grid. The AuNPs will be used in the alignment of the tomographic tilt series. To protect the specimen from beam-induced damage during the long exposure time needed for tomography data acquisition, the acquisition of the tomographic tilt series was performed at liquid nitrogen temperature on a Krios G4 (ThemoFisher™) electron microscope. The real temperature at the stage level was around −183° C. The tilt series was acquired in energy-filtered (EF) mode using a 30 eV slit for increasing the contrast of bright field TEM images. The detection was done on the Falcon i electron direct detector camera run in electron counting mode with 4096-pixel frame size. To keep the total exposure dose low, only the sample tracking was performed after each tilt series during data acquisition. The re-focusing was performed manually around every 10 images. The angular range was ±64° with a tilt step of 1°. The tilt series were aligned in the IMOD software using 13 AuNPs as fiducial markers that were clearly visible at each tilting angle. Prior to the reconstruction an image binning of 2 was performed to increase the SNR and reduce the computation time. To enhance the visibility of the pores in the 3D tomograph the images were filtered using an average background subtraction filter (ABSF) implemented as a script in Digital Micrograph. The SIRT reconstruction algorithm run with 100 iterations and a relaxation coefficient of 1 was employed.

[0093] Example 1A: A quantity of 2.4 grams of NH_4OH was added to 28.3 grams of water while stirring. To this solution, a quantity of 1.0 grams of dried zeolite HY-15 was dispersed and further stirred for 0.25 hours. Then, a quantity of 0.4 grams of CTAB was added and further stirred for hours. The resultant solution was further stirred for 1 hour, followed by hydrothermal treatment at 130° C. for 24 hours. The resulting solids were filtered, washed with water, and dried at 120° C. for 24 hours. The synthesized products were calcined in air at 550° C. for 6.0 hours at a ramp rate of 60° C./hour to yield AH-CT (where AH refers to ammonium hydroxide and CT refers to CTAB). The AH-CT synthesized in accordance this procedure exhibits disordered mesoporosity, and is characterized in FIGS. **3**A-**4**B, with an SEM image presented in FIG. **6** and structural and textural properties provided in Table 3.

[0094] In an alternative procedure, a quantity of 2.0 grams of dried zeolite HY-15 was dispersed in 56.6 grams of water while stirring. To this solution, 0.77 grams of cetyltrimethylammonium bromide (CTAB) was added and further stirred for 0.5 hours. Subsequently, 4.75 grams of aqueous ammonium hydroxide (30 wt %) was added dropwise to the mixture under stirring. The resultant solution was further stirred for 0.5 hours, followed by hydrothermal treatment at 130° C. for 24 hours. The resulting solids were filtered, washed with water and dried at 120° C. for 24 hours. The synthesized products were calcined in air at 550° C. for 6.0 hours at a ramp rate of 60° C./hour to yield AH-CT, which exhibits disordered mesoporosity.

[0095] Example 1B: A procedure for synthesis of 2D-hexagonally ordered mesoporous FAU-type zeolites is provided. A quantity of 2.4 grams of NH_4OH was added to 28.3 grams of water while stirring. A quantity of 1.0 grams of dried zeolite HY-15 was dispersed in the base solution and further stirred for 0.25 hours. Then, a quantity of 1.5 milliliters of dimethyloctadecyl(3-trimethoxysilyl-propyl)-ammonium chloride (DOAC) (42.0 wt % in methanol) was added and further stirred for 0.5 hours. The resultant solution was further stirred for 1 hour, followed by hydrothermal treatment at 130° C. for 24 hours. The resulting solids were filtered, washed with water, and dried at 120° C. for 24 hours. The synthesized products were calcined in air at 550° C. for 6.0 hours at a ramp rate of 60° C./hour to yield AH-TMS (where TMS refers to DOAC, dimethyloctadecyl (3-trimethoxysilyl-propyl)-ammonium chloride). The AH-TMS formed in accordance this procedure exhibits 2D-hexagonally ordered mesoporous symmetry, and is characterized in FIGS. **3**A-**4**B, with an SEM image presented in FIG. **6** and structural and textural properties provided in Table 3.

[0096] In an alternative procedure, a quantity of 2.0 grams of dried zeolite HY-15 was dispersed in 56.6 grams of water while stirring. To this dispersion, a quantity of 3.0 milliliters of organosilane, DOAC (42.0 wt % in methanol), was added and further stirred for 0.5 hours. Subsequently, 4.75 grams of aqueous ammonium hydroxide solution (30 wt %) was added dropwise to the mixture under stirring. The resultant solution was further stirred for 0.5 hours, followed by hydrothermal treatment at 130° C. for 24 hours. The resulting solids were filtered, washed with water and dried at 120° C. for 24 hours. The synthesized product was calcined in air at 550° C. for 6 hours with a ramp rate of 60° C./hour to yield AH-TMS. The AH-TMS formed in accordance with this procedure possesses 2D-hexagonally ordered mesoporous symmetry (as is apparent in the TEM images of this AH-TMS presented in FIGS. **5**A-**5**C).

[0097] Example 1C: A quantity of 0.6 grams of urea was added to 28.3 grams of water to form a homogeneous solution. To this solution, a quantity of 1.0 grams of dried zeolite HY-15 was dispersed and further stirred for 0.5 hours. Subsequently, 20 milliliters of water and 1.5 milliliters of DOAC (42.0 wt % in methanol) were added and further stirred for 2 hours. The resultant solution was subjected to hydrothermal treatment at 130° C. for 5 days. The resulting solids were filtered, washed with water, and dried at 120° C. for 24 hours. The synthesized products were calcined in air at 550° C. for 6.0 hours at a ramp rate of 60° C./hour to yield U-TMS (where U refers to urea). The U-TMS formed in accordance this procedure exhibits poorly defined mesoporosity, and is characterized in FIGS. **3**A-**4**B, with an SEM image presented in FIG. **6** and structural and textural properties provided in Table 3.

[0098] In an alternative procedure, a quantity of 1.2 grams of urea was dissolved in 60.0 grams of water to form a homogeneous solution. To this mixture, 2.0 grams of dried zeolite HY-15 was added and stirred for 10 minutes. Subsequently, 3.0 milliliters of DOAC (42.0 wt % in methanol) was added. The resulting solution was stirred for 0.5 hours, followed by hydrothermal treatment at 130° C. for 72 hours. The resulting mixture was filtered, washed with water and dried at 120° C. for 24 hours. The synthesized products were calcined in air at 550° C. for 6 hours with a ramp rate of 60° C./hour to yield U-TMS, which did not possess defined mesoporosity.

[0099] The calcined products from Examples 1A-1C and the reference HY-15 zeolite are characterized in FIGS. **3**A-**4**B, in which: FIG. **3**A depicts low-angle XRD patterns and FIG. **3**B depicts high-angle XRD patterns with intensity expressed in arbitrary units (a.u.) plotted against frequency 2θ(°); FIG. **4**A depicts N_2 physisorption isotherms plotting N_2 adsorbed ($cm^3 \cdot g^{-1}$) against relative pressure (P/P_0); and FIG. **4**B depicts non-local density functional theory (NLDFT) pore-size distributions plotting dV/d log W ($cm^3 \cdot g^{-1}$) (wherein "a" corresponds to commercial-USY (Zeolite HY-15), "b" corresponds to AH-CT, "c" corresponds to AH-TMS and "d" corresponds to U-TMS). In the Example 1B, the product hierarchically ordered zeolites are 2D-hexagonally ordered mesoporous FAU-type zeolites, having mesoporous channels, arranged in a hexagonal manner, as observed in the [100] and [110] directions with FAU micropore channels in the walls and mass of the mesostructure between mesopores.

[0100] FIGS. **5**A-C are TEM micrographs of calcined AH-TMS (formed according to the alternative procedure in Example 1B) showing hexagonal mesoporous channels in the and [110] directions, wherein: FIG. **5**A shows the TEM micrograph at a scale of 50 nanometers; FIG. **5**B shows the TEM micrographs in the [100] direction and in the [110] direction at a scale of 20 nanometers, and also depicts corresponding schematic diagrams and unit cell dimensions; and FIG. **5**C shows the TEM micrograph in the [100] direction at a scale of 10 nanometers (with an overlaying schematic diagram of the underlying zeolite structure).

[0101] FIG. **6** shows SEM images of (A) parent zeolite, HY-15; and the calcined products herein, (B) AH-CT, (C) AH-TMS and (D) U-TMS. The image (B) for AH-CT does not indicate notable changes in the morphology even at the crystal edges, whereas the image for AH-TMS does indicate

changes in the morphology indicative of functionality of the organosilanes, possessing a bulkier head and silanol groups than CTAB, resulting in improved dissolution and reassembly. Regarding the U-TMS, the urea-mediated synthesis improved the crystallinity considerably (image (D) in FIG. **6**) but the mesoporous structure was poorly defined as is apparent in pattern (d) of FIG. **3**A. While not wishing to be bound by theory it, these contrasting results suggest that the rate of dissolution influences not only recrystallization but also supramolecular self-assembly. Mesophase organization can be influenced by numerous physicochemical phenomena, including Coulombic interactions between organic and inorganic species, hydration energy, and hydrophobic effect. In the absence of strong alkali cations, surfactant-zeolite interactions play a key role in promoting cooperative self-assembly to induce the mesophase. In the case of AH-TMS, the zeolite dissolution was instantaneous, and importantly, the —$Si(OCH_3)_3$ groups on the organosilane head group can readily hydrolyze to interact with anionic zeolitic components to promote mesophase. Conversely, in the case of U-TMS, the concentration of anionic inorganic components changes gradually over time, thus progressively varying the charge balance at the micellar interface, disrupting the mesophase formation.

[0102] The high-degree of long-range ordering is apparent from the low-angle XRD pattern "c" of FIG. **3**A exhibiting Bragg's reflections at angles corresponding to 100, 110 and 200 planes, indicative of hexagonal mesopore symmetry in the AH-TMS. Conversely, in Example 1A, the use of relatively smaller templates or surfactant molecules (CTAB) causes diffusion inside the zeolitic pores causing inhomogeneous dissolution and preventing comprehensive reorganization. This is apparent from the low-angle XRD patterns "b" and "d" which did not exhibit a high-degree of long-range ordering despite having a uniform pore size distribution (PSD) from the corresponding N_2 physisorption isotherm (FIG. **4**A), attributed to non-homogeneous zeolite dissolution and restricted supramolecular self-assembly. The retention of the underlying zeolite structure is apparent from the high-angle XRD patterns of FIG. **3**B which are consistent with those for the parent zeolite, FAU zeolite, for all samples. In addition, AH-TMS demonstrates excellent hierarchically ordered mesoporosity as indicated by characteristic type-IV isotherm with H1 hysteresis (FIG. **4**A). Further, a high mesopore volume and narrow pore-size distribution further supports the presence of long-range ordered mesoporosity (FIG. **4**B).

[0103] Example 2A: A procedure for synthesis of 3D-cubic ordered mesoporous FAU-type zeolites is provided. A quantity of 0.6 grams of urea was added to 10.0 grams of water to form a homogeneous solution. To this solution, a quantity of 1.0 grams of dried zeolite HY-15 was added and stirred for 0.5 hours. Subsequently, 20 milliliters of water, 0.1 grams of ammonium nitrate (NH_4NO_3) as a source of ionic co-solute and 1.5 milliliters of DOAC (42.0 wt % in methanol) were added stepwise and the mixture further stirred for 2 hours. The resultant solution was subjected to hydrothermal treatment at 130° C. for 5 days. The resulting solids were filtered, washed with water, and dried at 120° C. for 24 hours. The synthesized products were calcined in air at 550° C. for 6.0 hours at a ramp rate of 60° C./hour to yield U-N-TMS-130 (where N refers to nitrate and "130" refers to the hydrothermal treatment temperature). The U-N-TMS-130 formed in accordance with this procedure exhibits 3D-cubic ordered mesoporous symmetry, and is characterized in FIGS. **7**A-**8**B, with a TEM image presented in FIG. **9** and structural and textural properties provided in Table 3.

[0104] In an alternative procedure, a quantity of 1.2 grams of urea was dissolved in 60.0 grams of water to form a homogeneous solution. To this mixture, 0.2 grams of ammonium nitrate (NH_4NO_3) was added as a source of ionic co-solute, and stirred to form a homogeneous solution. 2.0 grams of zeolite HY-15 was added and stirred for 10 minutes. Subsequently, 3.0 milliliters of DOAC (42.0 wt % in methanol) was added. The resulting solution was stirred for 0.5 hours, followed by hydrothermal treatment at 130° C. for 72 hours. The resulting solids were filtered, washed with water and dried at 120° C. for 24 hours. The synthesized product was calcined in air at 550° C. for 6 hours with a ramp rate of 60° C./hour to yield U-N-TMS. The calcined U-N-TMS formed in accordance with this procedure exhibits 3D-cubic ordered mesoporous symmetry, as is apparent in the TEM images presented in FIGS. **10**A-**10**B.

[0105] Example 2B: A procedure similar to that identified herein in the first procedure of Example 2A was followed, except that 1.0 grams of urea and 2.0 milliliters of DOAC (42.0 wt % in methanol) were used, and hydrothermal treatment was carried out at 150° C. for 72 hours. The calcined product is U-N-TMS-150 that possessed 3D-cubic ordered mesoporous symmetry. The U-N-TMS-150 from this procedure is characterized in FIGS. **7**A-**8**B, and its TEM images are presented in FIG. **12** and structural and textural properties provided in Table 3.

[0106] The calcined mesoporous zeolite products from Examples 2A and 2B, and the reference HY-15 zeolite, are characterized in FIGS. **7**A-**8**B, in which: FIG. **7**A depicts low-angle XRD patterns and FIG. **7**B depicts high-angle XRD patterns with intensity expressed in arbitrary units (a.u.) plotted against frequency 2θ(°); FIG. **8**A depicts N_2 physisorption isotherms plotting N_2 adsorbed ($cm^3 \cdot g^{-1}$) against relative pressure (P/P_0); and FIG. **8**B depicts non-local density functional theory (NLDFT) pore-size distributions plotting dV/d log W ($cm^3 \cdot g^{-1}$) (wherein "a" corresponds to commercial-USY (Zeolite HY-15), "b" corresponds to U-N-TMS-130 and "c" corresponds to U-N-TMS-150). In the Examples 2A and 2B, the product hierarchically ordered zeolites are 3D-cubic ordered mesoporous FAU-type zeolites, having cubic mesoporous channels present in the [100] and [110] directions with FAU micropore channels in the walls and mass of the mesostructure between mesopores.

[0107] FIG. **9** presents TEM micrographs of calcined U-N-TMS-130 formed according to the first procedure of Example 2A, showing cubic mesoporous channels in the [111] and [110] directions, wherein image (A) in the [111] direction at a scale of 100 nanometers, and images (B) and (C) are in the [112] direction at a scale of 50 nanometers (with image (B) enlarged relative to image (C)). FIGS. **10**A-B are TEM micrographs of calcined U-N-TMS formed according to the second procedure of Example 2A showing cubic mesoporous channels in the [111] and [110] directions, wherein: FIG. **10**A shows the TEM micrograph at a scale of 100 nanometers; FIG. **10**B shows the TEM micrograph in the [110] direction and in the [111] direction at a scale of 20 nanometers; and FIG. **10**C depicts a FAU unit cell schematic and dimensions and their arrangement to provide long-range mesoporous ordering. The high-degree of long-range ordering is apparent from the low-angle XRD patterns of FIG. **7**A,

exhibiting Bragg's reflections 211, 220, 321, 400, 420 and 332, which are characteristic of bicontinuous gyroid (cubic) (Ia-3d) mesopore symmetry (where the reflections at 321, 400, 420 and 332 are magnified). The retention of the underlying zeolite structure is apparent from the high-angle XRD patterns of FIG. **7**B, which are consistent with those for the parent zeolite, FAU zeolite. In addition, the U-N-TMS-130 and U-N-TMS-150 demonstrate excellent hierarchically ordered mesoporosity as indicated by characteristic type-IV isotherm with H1 hysteresis depicted in the N2 physisorption isotherms of FIG. **8**A. Further, a high mesopore volume and narrow pore-size distribution demonstrated in FIG. **8**B further supports the presence of long-range ordered mesoporosity. FIG. **11** presents an electron tomography reconstruction of U-N-TMS-150 with an inset to magnify the pore architecture and show an overlay diagram of the structure. FIG. **12** presents TEM micrographs of U-N-TMS-150 with corresponding structural diagrams, with image (A) showing TEM micrograph at a scale of 20 nanometers in the [100] orientation, image (B) showing a scale of 50 nanometers in the orientation and image (C) showing a scale of 10 nanometers in the [111] orientation, with insets in (A) and (B) showing magnified images and the inset in (C) showing selected area electron diffraction (SAED). The U-N-TMS-150 synthesized at a higher temperature demonstrated improved textural properties as a result of the thorough removal of non-framework aluminum. The 3D mesostructure by electron tomography (ET) revealed a homogenous distribution of mesoporous channels inside the zeolite volume. A longitudinal slice cut through the middle of the zeolite grain shows a continuous network of mesopores developed along a single crystallographic direction. The inset in FIG. **11** highlights the 3D spatial homogeneity of the hierarchical pore architecture. The interconnected mesopore network formed by the zeolite framework extends from the zeolite grain external facets to its core.

[0108] In addition, when comparing the products of Example 1C (U-TMS) with that of Examples 2A and 2B (U-N-TMS), the benefit of the ionic co-solute contribution of the nitrate is apparent. The ionic co-solute serves to influence the cubic micelle shape by the Hofmeister effect, around with the FAU-type zeolite oligomers are arranged. In the Example 1C there is a degree of periodicity of mesopore arrangement possibly from either a bimodal system or a structure collapse, however, there is a significant lack of any long-range ordering as compared with the products of Examples 2A and 2B having the nitrate anion where it is observed by low angle XRD showing reflections characteristic of gyrodial bicontinuous (cubic) mesopore structure (Ia-3d).

[0109] Example 3A: A procedure for synthesis of 2D-hexagonally ordered mesoporous FAU-type zeolites is provided using a sulfate as an ionic co-solute. A quantity of 0.6 grams of urea was added to 10.0 grams of water to form a homogeneous solution. To this solution, a quantity of 1.0 grams of dried zeolite HY-15 was added and stirred for 0.5 hours. Subsequently, 20 milliliters of water, 0.165 grams of ammonium sulfate ($(NH_4)_2SO_4$) and 1.5 milliliters of DOAC (42.0 wt % in methanol) were added stepwise and the mixture further stirred for 2 hours. The resultant solution was subjected to hydrothermal treatment at 130° C. for 72 hours. The resulting solids were filtered, washed with water, and dried at 120° C. for 24 hours. The synthesized products were calcined in air at 550° C. for 6.0 hours at a ramp rate of 60° C./hour to yield U-S-TMS (where U refers to urea, S refers to sulfate and TMS refers to DOAC). The U-S-TMS formed in accordance this procedure exhibit 2D-hexagonally ordered mesoporous symmetry, and is characterized in FIGS. **13**A-**14**B, with TEM images presented in FIG. **15** and structural and textural properties provided in Table 3.

[0110] In an alternative procedure, a quantity of 1.2 grams of urea was dissolved in 60.0 grams of water to form a homogeneous solution. To this mixture, a quantity of 0.33 grams of ammonium sulfate $(NH_4)_2SO_4$ was added as a source of ionic co-solute, and stirred until homogeneous. Thereafter a quantity of 2.0 grams of dried zeolite HY-15 was added and stirred for 10 minutes. Subsequently, 3.0 milliliters of DOAC (42.0 wt % in methanol), was added. The resulting solution was stirred for 0.5 hours, followed by hydrothermal treatment at 130° C. for 72 hours. The resulting solids were filtered, washed with water and dried at 120° C. for 24 hours. The synthesized product was calcined in air at 550° C. for 6 hours with a ramp rate of 60° C./hour to yield U-S-TMS, which possesses 2D-hexagonally ordered mesoporous symmetry.

[0111] Example 3B: A procedure for synthesis of 2D-lamellar ordered mesoporous FAU-type zeolites is provided using a perchlorate as an ionic co-solute. A quantity of 0.6 grams of urea was added to 10.0 grams of water to form a homogeneous solution. To this solution, a quantity of 1.0 grams of dried zeolite HY-15 was added and stirred for 0.5 hours. Subsequently, 20 milliliters of water, 0.46 grams of sodium perchlorate ($NaClO_4$) and 1.5 milliliters of DOAC (60.0 wt % in methanol) were added stepwise and the mixture further stirred for 2 hours. The resultant solution was subjected to hydrothermal treatment at 130° C. for 72 hours. The resulting solids were filtered, washed with water, and dried at 120° C. for 24 hours. The synthesized products were calcined in air at 550° C. for 6.0 hours at a ramp rate of 60° C./hour to yield U-C-TMS (where U refers to urea, C refers to perchlorate and TMS refers to DOAC). The as-made U-C-TMS formed in accordance this procedure exhibit 2D-lamellar ordered mesoporous symmetry. The as-made and calcined U-C-TMS are characterized in FIG. **13**A. The calcined U-C-TMS is characterized in FIG. **13**B, **14**A-**14**B and structural and textural properties provided in Table 3.

[0112] When comparing the Examples 3A and 3B, the influence of the anion selection is apparent. An ionic co-solute selection of perchlorate influenced a lamellar micelle shape whereas an ionic co-solute selection of nitrate influenced a cubic micelle shape by the Hofmeister effect. In both examples, the FAU-type zeolite oligomers are arranged around the shaped micelles.

[0113] The as-made and calcined products from Examples 3A-3B are characterized in FIG. **13**A, and the calcined products from Examples 3A-3B are characterized in FIGS. **13**B and **13**A-**13**B (wherein "a" corresponds to U-S-TMS and "b" corresponds to U-C-TMS). FIG. **13**A depicts low-angle XRD patterns and FIG. **13**B depicts high-angle XRD patterns with intensity expressed in arbitrary units (a.u.) plotted against frequency 2θ(°), with as-made patterns shown in dashed lines and calcined patterns shown in solid lines. FIG. **14**A depicts N2 physisorption isotherms plotting N_2 adsorbed ($cm^3 \cdot g^{-1}$) against relative pressure (P/P_0), and FIG. **14**B depicts non-local density functional theory (NLDFT) pore-size distributions plotting dV/d log W

($cm^3 \cdot g^{-1}$). The high-degree of long-range ordering of as-made and calcined U-S-TMS is apparent from FIG. **13**A, where low-angle XRD patterns exhibit Bragg's reflection peaks 100, 110 and 200, indicative of 2D-hexagonally ordered mesoporous symmetry. The high-degree of long-range ordering of as-made U-C-TMS is also apparent FIG. 13A, with Bragg's reflection peaks 100 and 200 indicative of 2D-lamellar (p2) mesopore symmetry, but this ordering is lost as the structure collapsed during calcination. The retention of the underlying zeolite structure is apparent from FIG. **13**B, where high-angle XRD patterns are consistent with those for the parent zeolite, FAU zeolite.

[0114] FIG. **15** presents TEM micrographs of the U-S-TMS synthesized in the first procedure of Example 3A, including image (A) at a scale of 20 nanometers with a corresponding structural diagram, image (B), an enlarged view of a portion of the image (A) with a fast Fourier transform pattern inset, image (C) at a scale of 50 nanometers showing selected area electron diffraction (SAED) in the inset, image (D) at 50 nanometers, and image (E) at 20 nanometers with a corresponding structural diagram.

[0115] Example 4A: A procedure for synthesis of 2D-lamellar ordered mesoporous FAU-type zeolites is provided. A quantity of 1.2 grams of urea was dissolved in 60.0 grams of water to form a homogeneous solution. To this mixture, 2.0 grams of zeolite HY-15 was added and stirred. 0.92 grams of sodium perchlorate ($NaClO_4$) was added and stirred for 10 minutes. Subsequently, 3.0 milliliters of an DOAC (42.0 wt % in methanol) was added. The resulting solution was stirred for hours, followed by hydrothermal treatment at 130° C. for 72 hours. The resulting solids were filtered, washed with water and dried at 120° C. for 24 hours. The synthesized product was calcined in air at 550° C. for 6 hours with a ramp rate of 60° C./hour to yield U-C-TMS (in which Y refers to zeolite Y, C refers to perchlorate, U refers to urea and TMS refers to DOAC). The as-made U-C-TMS formed in accordance this procedure exhibit 2D-lamellar ordered mesoporous symmetry, and is characterized in FIGS. **16**A-B, with TEM images presented in FIGS. **17**A-**17**C.

[0116] Example 4B: A procedure follows that of Example 4A, except that a quantity of 4.75 grams of NH_4OH is used as the alkaline reagent instead of urea.

[0117] In the Example 4A, the product hierarchically ordered zeolite is a 2D-lamellar ordered mesoporous FAU-type zeolite, having lamellar mesoporous channels present in the [100] direction with FAU micropore channels in the walls and mass of the mesostructure between mesopores. FIG. **16**A depicts low-angle XRD patterns and FIG. **16**B depicts high-angle XRD patterns, wherein "a" corresponds to commercial-USY (Zeolite HY-15) and "b" corresponds to U-C-TMS: FIGS. **17**A-C depict the U-C-TMS lamellar structures, wherein: FIG. **17**A shows the TEM micrograph at a scale of 50 nanometers in a planar orientation [100]; FIG. **17**B shows the TEM micrograph at a scale of 20 nanometers; and FIG. **17**C shows the TEM micrograph at a scale of 50 nanometers in a planar orientation [110]. The high-degree of long-range ordering is apparent from FIG. **16**A, where low-angle XRD patterns exhibit Bragg's reflection peaks 100 and 200 indicative of 2D-lamellar (p2) mesopore symmetry. The retention of the underlying zeolite structure is apparent from FIG. **16**B, where high-angle XRD patterns are consistent with those for the parent zeolite, FAU zeolite.

[0118] According to the examples herein, hierarchically ordered FAU-type frameworks exhibiting 2D-hexagonal (p6 mm), 3D-cubic (Ia-3d) and 2D-lamellar (p2) mesopore symmetries are prepared for the first time by a methodical post-synthetic reassembly.

[0119] Example 5—Acidity Characterization: Acid site characterization of was carried out by Fourier-transform infrared spectroscopy (FTIR) using a Nicolet 6700 spectrophotometer with pyridine as the probe molecule. Before the analysis, pelletized samples were degassed at 450° C. under vacuum (10^{-5} mbar) for 24 h. After cooling down to room temperature, the pyridine vapors were dosed for 0.5 h periodically. Subsequently, the physisorbed pyridine was removed under vacuum at 150° C. for 2 h before recording the FTIR spectra. Acid site quantification was done using the following formulae

$$C_{BAS}=\mathrm{IMEC}_{BAS}{}^{-1}\times IA_{BAS}\times\pi R^2/W$$

$$C_{LAS}=\mathrm{IMEC}_{LAS}{}^{-1}\times IA_{LAS}\times\pi R^2/W$$

where C is the concentration (μmol/g zeolite) of acid sites (BAS—Brønsted acid site and LAS—Lewis acid site), $IMEC_{BAS}$, and $IMEC_{LAs}$ refers to the integrated molar extinction coefficients (BAS—1.67 cm/μmol; LAS—2.22 cm/μmol), IA_{BAS} and IA_{LAS} integrated absorbances (cm^{-1}), R (cm) and W (mg) are the radius and weight of zeolite pellet/disk.

[0120] FIG. **18** depicts FTIR spectra of the parent zeolite (a), and HOCMMs herein including the U-N-TMS-150 (b) and the U-S-TMS synthesized in the first procedure of Example 3A (c). Brønsted acid cites are indicated at wavenumber 1545 cm^{-1} and Lewis acid cites are indicated at wavenumber 1445 cm^{-1}. Table 4 shows acid properties of the parent zeolite, and the U-N-TMS-150 and U-S-TMS synthesized in the first procedure of Example 3A. The overall acidity of the HOCMMs synthesized is lower compared with the parent zeolite, attributed to the removal of non-framework-Al in the parent zeolite during the reassembly; framework-Al is present as Brønsted acid sites (0.28 mmol/g). The acid sites are reorganized and distributed in the HOCMMs as both new Lewis acid sites (~0.1 mmol/g) and Brønsted acid sites (~0.25 mmol/g). Despite having a lower concentration of zeolitic acid sites compared with the parent zeolite, the HOCMMs synthesized are effective as catalysts supports. The Brønsted/Lewis acid site ratios are higher for the HOCMMs synthesized compared to the parent zeolite.

[0121] Example 6—Additional characterization: Additional properties of the parent zeolite (a), and HOCMMs herein including the U-N-TMS-150 (b) and the U-S-TMS synthesized in the first procedure of Example 3A (c), were determined using ^{29}Si MAS-NMR and ^{27}Al MAS-NMR spectroscopy, shown in FIGS. **19**A-B. The ^{29}Si-NMR spectra (FIG. **19**A) show two major resonances at ~106 ppm and ~101 ppm corresponding to silicon atoms in 4Si(0Al) and 3Si(1Al) environments, namely Q^4 and $Q^{3'}$ silica, respectively. The Si/Al ratios calculated from ^{29}Si-NMR spectra (14.8) and inductively coupled plasma analysis (Si/Al~8.9) revealed that the parent zeolite has nearly 40% of its aluminum as non-framework species in octahedral coordination, which can be seen as a sharp resonance (AlO) at '~0 ppm' in the ^{27}Al-NMR spectra (FIG. **19**B). The presence of a high non-framework-Al can be detrimental in catalytic reactions as it causes micropore blockage and alters the product selectivity and coke composition. Conversely, the

HOCMMs characterized herein exhibit a higher concentration of framework-Al atoms in the tetrahedral coordination (Al_T) as seen by a broad resonance at '~60 ppm'. In particular, the U-N-TMS-130 pattern (b) exhibits 'Al' atoms predominantly in the Td coordination. Without wishing to be bound by theory it is expected that this is due to exhaustive dealumination at high synthesis temperatures. Without wishing to be bound by theory the broadness of the Al_T resonance associated with the HOZ materials can be ascribed to slight changes in the Al—O bond lengths due to renewed periodicity, aluminum distribution, and crystallite size of the zeolite frameworks.

[0122] Example 6—Base-mediated dissolution/incision: Base-mediated dissolution studies of the parent zeolite were performed at 130° C. in the absence of a surfactant to interpret the nature of the hierarchical ordering by post-synthetic ensembles process to promote reorganization at the unit-cell level. FIGS. **20**A and **20**B depict high-angle XRD patterns of the parent zeolite in various stages of treatment. In FIG. **20**A, the patterns are the parent zeolite, and after treatment at 130° C. for 1.5 hours with NH_4OH and urea, FIG. **20**B depicts the parent zeolite treated with urea at 130° C. after 1.5 hours, 6 hours and 18 hours. FIG. **20**C depicts 29 Si MAS-NMR and FIG. **20**D depicts ^{27}Al MAS-NMR spectra of (a) HY-15; (b) after NH_4OH treatment at 130° C./1.5 h; (c) after urea-treatment at 130° C./6h. The high-angle XRD studies (FIGS. **20**A-B) reveal that, while NH_4OH almost dissolves the zeolite to amorphous frameworks in 1.5 h, urea treatment resulted in partial dissolution even after 6 h. The ^{27}Al- and ^{29}Si-magic angle spinning-nuclear magnetic resonance (MAS-NMR) spectra (FIGS. **20**C-D) suggest that the urea treatment selectively dissolves Si—O—Si bonds without strongly affecting the 'Si—O—Al' regions and thus the majority of the aluminum is still inside the framework in tetrahedral coordination (Al_T~60 ppm). Such dissolution patterns can result in oligomeric zeolitic fragments (Q^{4a}, $Q^{3'}$, Al_T) with siloxane (Q^{4b}) or silanol extensions (Q^3), which can be readily reorganized into crystalline mesostructures during thermal treatments. The formation of such zeolite fragments (FIG. **20**E) is a factor in the hierarchical ordering by post-synthetic ensembles process to fabricate HOCMMs. Without wishing to be bound by theory it is expected that, in the presence of surfactants, the quantity of Q^{4b} and Q^3 species can be significantly fewer due to the surfactant-zeolite interactions that restrict over-dissolution.

[0123] In the case of base-mediated reassembly, zeolite dissolution can result in partially crystalline oligomers, which can be recrystallized during hydrothermal (synthesis) and thermal treatments (calcination). However, an uncontrolled dissolution can result in isolated amorphous domains, which fail to recrystallize due to the absence of suitable conditions (high alkalinity and inorganic cations). Therefore, a high concentration of strong bases such as NaOH and NH_4OH can result in uncontrolled dissolution to form amorphous components causing pore-blockage and a concentration gradient across the zeolite crystals. Low base concentrations can lead to insufficient zeolite dissolution due to the decrease in the base concentration with time. As a result, strategically controlling the zeolite dissolution is a factor to enable reassembly into crystalline mesostructures in the syntheses processes herein for HOCMMs.

[0124] As used herein, the phrase "a major portion" with respect to a particular composition and/or solution and/or other parameter means at least about 50% and up to 100% of a unit or quantity. As used herein, the phrase "a significant portion" with respect to a particular composition and/or solution and/or other parameter means at least about 75% and up to 100% of a unit or quantity. As used herein, the phrase "a substantial portion" with respect to a particular composition and/or solution and/or other parameter means at least about 90, 95, 98 or 99% and up to 100% of a unit or quantity. As used herein, the phrase "a minor portion" with respect to a particular composition and/or solution and/or other parameter means at least about 1, 2, 4 or 10%, up to about 20, 30, 40 or 50% of a unit or quantity.

[0125] It is to be understood that like numerals in the drawings represent like elements through the several figures, and that not all components and/or steps described and illustrated with reference to the figures are required for all embodiments or arrangements. Further, the terminology used herein is for the purpose of describing particular embodiments only and is not intended to be limiting of the invention. As used herein, the singular forms "a," "an" and "the" are intended to include the plural forms as well, unless the context clearly indicates otherwise. It will be further understood that the terms "including," "comprising," "having," "containing," "involving," and variations thereof herein, when used in this specification, specify the presence of stated features, integers, steps, operations, elements, and/or components, but do not preclude the presence or addition of one or more other features, integers, steps, operations, elements, components, and/or groups thereof.

[0126] It should be noted that use of ordinal terms such as "first," "second," "third," etc., in the claims to modify a claim element does not by itself connote any priority, precedence, or order of one claim element over another or the temporal order in which acts of a method are performed, but are used merely as labels to distinguish one claim element having a certain name from another element having a same name (but for use of the ordinal term) to distinguish the claim elements.

[0127] Notably, the figures and examples above are not meant to limit the scope of the present disclosure to a single implementation, as other implementations are possible by way of interchange of some or all the described or illustrated elements. Moreover, where certain elements of the present disclosure can be partially or fully implemented using known components, only those portions of such known components that are necessary for an understanding of the present disclosure are described, and detailed descriptions of other portions of such known components are omitted so as not to obscure the disclosure. In the present specification, an implementation showing a singular component should not necessarily be limited to other implementations including a plurality of the same component, and vice-versa, unless explicitly stated otherwise herein. Moreover, applicants do not intend for any term in the specification or claims to be ascribed an uncommon or special meaning unless explicitly set forth as such. Further, the present disclosure encompasses present and future known equivalents to the known components referred to herein by way of illustration.

[0128] The foregoing description of the specific implementations will so fully reveal the general nature of the disclosure that others can, by applying knowledge within the skill of the relevant art(s), readily modify and/or adapt for various applications such specific implementations, without undue experimentation, without departing from the general

concept of the present disclosure. Such adaptations and modifications are therefore intended to be within the meaning and range of equivalents of the disclosed implementations, based on the teaching and guidance presented herein. It is to be understood that the phraseology or terminology herein is for the purpose of description and not of limitation, such that the terminology or phraseology of the present specification is to be interpreted by the skilled artisan in light of the teachings and guidance presented herein, in combination with the knowledge of one skilled in the relevant art(s). It is to be understood that dimensions discussed or shown are drawings accordingly to one example and other dimensions can be used without departing from the disclosure.

[0129] The subject matter described above is provided by way of illustration only and should not be construed as limiting. Various modifications and changes can be made to the subject matter described herein without following the example embodiments and applications illustrated and described, and without departing from the true spirit and scope of the invention encompassed by the present disclosure, which is defined by the set of recitations in the following claims and by structures and functions or steps which are equivalent to these recitations.

TABLE 1

Crystal systems.

System	Unit cell	Essential symmetry of crystal
Triclinic	No special relationship	None
Monoclinic	$a \neq b \neq c$	Two-fold axis or mirror plane
	$\alpha = \gamma = 90° \neq \beta$	(inverse two-fold axis)
Orthorhombic	$a \neq b \neq c$	Three orthogonal two-fold or
	$\alpha = \beta = \gamma = 90°$	inverse two-fold axes
Tetragonal	$a = b \neq c$	One four-fold or inverse four-
	$\alpha = \beta = \gamma = 90°$	fold axis
Trigonal	$a = b = c$	One three-fold axis or inverse
	$\alpha = \beta = \gamma \neq 90°$	three-fold axis
Hexagonal	$a = b \neq c$	One six-fold or inverse six-fold
	$\alpha = \beta = 90°, \gamma = 120°$	axis
Cubic	$a = b = c$	Four three-fold axes

TABLE 2

Crystal classes

	Crystal classes (point group)	
System	Non-centrosymmetric	Centrosymmetric
Triclinic	1	$\bar{1}$
Monoclinic	2, m (= $\bar{2}$)	2/m
Orthorhombic	222, 2 mm	mmm
Tetragonal	4, $\bar{4}$	4/m
	422, 4 mm, $\bar{4}2$ m	4/mmm
Trigonal	3	$\bar{3}$
	32, 3 m	$\bar{3}$ m
Hexagonal	6, $\bar{6}$	6/m
	622, 6 mm, $\bar{6}2$ m	6/mmm
Cubic	23	m$\bar{3}$
	432, $\bar{4}3$ m	m$\bar{3}$ m

TABLE 3

Structural and textural properties of hierarchical zeolites

	a_0 (nm)[Φ]		S_{BET} ($m^2 g^{-1}$)[a]		D	V_p ($cm^3 g^{-1}$)[d]		V_p –
Sample	micro[¢]	meso	Micro[b]	Total	(nm)[c]	Micro[b]	Total	Meso (%)[e]
U-N-TMS-150	24.39	10.1[¢]	374	964	4.4	0.15	0.75	80.0
U-N-TMS-130	24.36	10.1[¢]	430	846	4.2	0.18	0.59	69.4
U-S-TMS	24.40	5.2[¥]	386	825	4.4	0.16	0.57	71.9
U-C-TMS	24.22	4.1[¶]	531	763	—	0.21	0.48	0.56
HY-15	24.28	—	640	811	—	0.25	0.44	43.2
U-TMS	24.21	—	417	874	—	0.21	0.41	48.8
AH-TMS	24.34	5.1[¥]	207	699	4.7	0.10	0.57	82.4
AH-CT	24.37	—	275	612	—	0.11	0.49	77.5

[a]Brunauer-Emmett-Teller (BET) surface area;
[b]calculated using the t-plot method;
[c]mesopore size;
[d]pore volume;
[d]pore volume;
[e]percentage of mesopore volume.
[Φ]Unit-cell parameters calculated by formulae - [¢]$a = d\sqrt{(h^2 + k^2 + 1^2)}$; [¥]$a = 2d \cdot \sqrt{(h^2 + hk + k^2/3)}$;
[¶]calculated from as-synthesized x-ray diffraction pattern.

TABLE 4

Acid properties and catalytic activities

Zeolite	Si/Al[a]	BAS (mmol/g)	LAS (mmol/g)	Total (mmol/g)	B/L[b]
U-N-TMS-150	10.9	0.13	0.07	0.20	1.7
U-S-TMS	12.2	0.15	0.10	0.25	1.4
HY-15	14.8	0.28	0.44	0.72	0.6

[a]^{29}Si MAS-NMR;
[b]Brønsted/Lewis acid ratio

1. (canceled)

2. A method for synthesis of hierarchically ordered crystalline microporous material having a high-degree of long-range mesoporous ordering, the method comprising:

forming an aqueous suspension of an effective amount of a parent crystalline microporous material having an underlying microporous structure, an effective amount of an alkaline reagent and an effective amount of a supramolecular template,

hydrothermally treating the aqueous suspension under conditions effective for mesophase transition to dis-

solve/incise parent crystalline microporous material into oligomeric units of the parent crystalline microporous material, form shaped micelles of the supramolecular template, and reorganize the oligomeric units around the shaped micelles into hierarchically ordered meso structures.

3. The method as in claim **2**, wherein the shape of the micelles is tuned by selection of the supramolecular template.

4. (canceled)

5. The method as in claim **2**, wherein the aqueous suspension further comprises an ionic co-solute that is separate from an anion associated with the supramolecular template, and wherein the shape of the micelles is tuned by selection of the supramolecular template and the ionic co-solute, wherein the ionic co-solute is selected from the group consisting of $CO3_2^-$, SO_4^{2-}, $S2O_3^{2-}$, $H_2PO_4^-$, F^-, Cl^-, Br^-, NO_3^-, I^-, ClO_4^-, SCN^- and $C_6H_5O_8^{-3}$.

6. The method as in claim **4**, wherein the ionic co-solute is selected from the group consisting of SO_4^{2-}, NO_3^-, and ClO_4^-.

7. The method as in claim **2**, wherein the aqueous suspension further comprises an ionic co-solute that is separate from an anion associated with the supramolecular template, and wherein the shape of the micelles is tuned by selection of the supramolecular template and the ionic co-solute, wherein the ionic co-solute comprises NO_3^- and wherein the hierarchically ordered mesostructures possess a cubic mesophase symmetry.

8. The method as in claim **7**, wherein the hierarchically ordered mesostructures possess a cubic mesophase symmetry and the mesophase transition is characterized by a surfactant packing parameter g in the range of about 0.4-0.8, wherein

$$g=V/a_0l$$

wherein

V=total volume of surfactant tails of the supramolecular template,

a_0=area of the head group of the supramolecular template, and

l=length of surfactant tail of the supramolecular template.

9. The method as in claim **7**, wherein the hierarchically ordered mesostructures possess a cubic mesophase symmetry and a molar ratio of supramolecular template to co-solute is in the range of about 0.8-1.3.

10. The method as in claim **2**, wherein the aqueous suspension further comprises an ionic co-solute that is separate from an anion associated with the supramolecular template, and wherein the shape of the micelles is tuned by selection of the supramolecular template and the ionic co-solute, wherein the ionic co-solute comprises SO_4^{2-} and wherein the hierarchically ordered mesostructures possess a hexagonal mesophase symmetry.

11. The method as in claim **10**, wherein the hierarchically ordered mesostructures possess a hexagonal mesophase symmetry and the mesophase transitions is characterized by a surfactant packing parameter g in the range of about 0.4-0.6, wherein

$$g=V/a_0l$$

wherein

V=total volume of surfactant tails of the supramolecular template,

a_0=area of the head group of the supramolecular template, and

l=length of surfactant tail of the supramolecular template.

12. The method as in claim **10**, wherein the hierarchically ordered mesostructures possess a hexagonal mesophase symmetry and a molar ratio of supramolecular template to co-solute is in the range of about 0.8-1.3.

13. The method as in claim **4**, wherein the ionic co-solute comprises ClO_4^- and wherein the hierarchically ordered mesostructures possess a lamellar mesophase symmetry.

14. The method as in claim **13**, wherein the hierarchically ordered mesostructures possess a lamellar mesophase symmetry and the mesophase transitions is characterized by a surfactant packing parameter g in the range of about 0.9-1.1, wherein

$$g=V/a_0l$$

wherein

V=total volume of surfactant tails of the supramolecular template,

a_0=area of the head group of the supramolecular template, and

l=length of surfactant tail of the supramolecular template.

15. The method as in claim **13**, wherein the hierarchically ordered mesostructures possess a lamellar mesophase symmetry and a molar ratio of supramolecular template to co-solute is in the range of about 0.2-0.7.

16-21. (canceled)

22. The method as in claim **2**, wherein the supramolecular templates are bulky surfactants having one or more dimensions larger than dimensions of micropores of the crystalline microporous material to constrain diffusion into micropores of the crystalline microporous material, wherein the dimensions relate to a head group of a surfactant, a tail group of a surfactant, or a co-template, wherein the supramolecular template contains at least one quaternary ammonium group, and at least one head group moiety selected from the group consisting of organosilanes, hydroxysilyls, alkoxysilyls, aromatics, branched alkyls, sulfonates, carboxylates, phosphates and combinations comprising one of the foregoing moieties, wherein an alkyl group bridging at least one of the quaternary ammonium groups and at least one of the head groups contains 1-10 carbon atoms.

23. The method as in claim **2**, wherein the supramolecular template comprises dimethyloctadecyl(3-trimethoxysilyl-propyl)-ammonium or a derivative of dimethyloctadecyl(3-trimethoxysilyl-propyl)-ammonium, wherein the supramolecular templates is a bulky surfactant having one or more dimensions larger than dimensions of micropores of the crystalline microporous material to constrain diffusion into micropores of the crystalline microporous material, wherein the dimensions relate to a head group of the surfactant.

24. The method as in claim **2**, wherein the alkaline reagent is provided at a concentration in the aqueous suspension of about 0.1-5 wt % and is selected from the group consisting of ammonia, ammonium hydroxide and urea.

25. The method as in claim **2**, wherein the alkaline reagent is urea, wherein during hydrothermal treatment, urea reacts to form ammonium hydroxide, thereby controlling hydrothermal treatment.

26. (canceled)

27. The method as in claim **2**, wherein the as-formed hierarchically ordered mesostructures are calcined, wherein calcining reduces amorphous content of the hierarchically ordered mesostructures.

28. The method as in claim **2**, wherein said parent crystalline microporous material comprises a zeolite or zeolite-type material.

29. The method as in claim **2**, wherein said parent crystalline microporous material is a zeolite having a framework selected from the group consisting of AEI, *BEA, CHA, FAU, MFI, MOR, LTL, LTA and MWW.

30. (canceled)

* * * * *